BRILL

Nematology 0 (2020) 1-30

Nematology
brill.com/nemy

Bursaphelenchus juglandis n. sp. (Nematoda: Aphelenchoididae), an associate of walnut twig beetle, *Pityophthorus juglandis*, the vector of thousand cankers disease

Alexander Y. RYSS [1,*], Corwin PARKER [2], Sergio ÁLVAREZ-ORTEGA [3], Steven A. NADLER [2] and Sergei A. SUBBOTIN [4,5]

[1] *Zoological Institute of the Russian Academy of Sciences, Universitetskaya Naberezhnaya 1, St Petersburg 199034, Russia*

[2] *Department of Entomology and Nematology, University of California, Davis, CA 95616, USA*

[3] *Departamento de Biología y Geología, Física y Química Inorgánica, Universidad Rey Juan Carlos, Campus de Móstoles, 28933-Madrid, Spain*

[4] *Plant Pest Diagnostic Center, California Department of Food and Agriculture, Sacramento, CA 95832-1448, USA*

[5] *Center of Parasitology of A.N. Severtsov Institute of Ecology and Evolution of the Russian Academy of Sciences, Leninskii Prospect 33, Moscow 117071, Russia*

Received: 31 March 2020; revised: 1 June 2020
Accepted for publication: 2 June 2020

Summary – *Bursaphelenchus juglandis* n. sp. was isolated from the walnut twig beetle, *Pityophthorus juglandis*, and walnut trees, *Juglans* spp. with symptoms of thousand cankers disease, in California, USA. Based on analysis of three rRNA genes and morphological features (three lines in lateral field, small arched vulval flap in female, broad spicule with two lines along blade and small cucullus, digitate dorsally bent condylus, male tail pattern of five papilliform papillae and one pair of glandpapillae (P5), and curved conical female tail), the new species belongs to the *Abietinus* group within *Bursaphelenchus*. It differs from similar species of this group by the presence of a cephalic disc with lateral labial sensilla at the disc border, and in having thick spicules with the capitulum surface almost parallel to a virtual direct line extending from the spicule end. An emended diagnosis, tabular polytomous identification key and compendium of species with the lists of their vectors, plant hosts, and distribution are provided for the *Abietinus* group. The diagnostics of the propagative developmental stages is given, including sex differences; the transmission dauer stage was identified as the third stage and its description given with sexual differences. A molecular phylogeny of *Bursaphelenchus* is provided based on partial 18S rRNA, ITS rRNA and the D2-D3 expansion fragments of 28S rRNA gene sequences. A PCR with a species-specific primer was developed for detection of *B. juglandis* n. sp.

Keywords – *Abietinus* group, *Geosmithia*, *Juglans*, key, molecular, morphology, morphometrics, new species, phylogeny, taxonomy, USA.

Bursaphelenchus contains over 125 nominal species (Ryss & Subbotin, 2017; Kanzaki & Giblin-Davis, 2018). Nematodes of this genus are mostly fungivores vectored by wood-inhabiting beetles of the families Curculionidae and Cerambycidae. Some *Bursaphelenchus* species are damaging pathogens of woody plants. *Bursaphelenchus xylophilus* (Steiner & Buhrer, 1934) Nickle, 1970 causes pine wilt disease in *Pinus* spp. and *B. cocophilus* (Cobb, 1919) Baujard, 1989 causes red ring disease in *Cocos nucifera* L. and *Elaeis guineensis* Jacq. In 2013-2019 during surveys of walnut (*Juglans* spp.) trees infected with the walnut twig beetle *Pityophthorus juglandis* Blackman, 1928 in California, USA, specimens of an unknown, putatively new *Bursaphelenchus* species were collected from the beetle vector and phloem of walnut trees with symptoms of thousand cankers disease (TCD) (Figs 1, 2).

A newly recognised disease of walnuts, TCD results from the combined activity of the beetle *P. juglandis* and a canker-producing fungus, *Geosmithia morbida* (Kolarik *et al*., 2011). The fungus often kills black walnut trees within 3 years of the development of symptoms. However, it may take several years after insect and

* Corresponding author, e-mail: alryss@gmail.com

DOI 10.1163/15685411-bja10037

Fig. 1. Thousand cankers disease. Dieback of *Juglans* sp., California, USA.

fungal attacks before symptoms are visible, starting with yellowing leaves and thinning of the tree crown. As the disease progresses, foliage wilts, larger branches and then eventually the entire tree dies (Tisserat *et al*., 2009).

The main goals of the present study were: *i*) to describe a new *Bursaphelenchus* species associated with walnut twig bark beetle, *P. juglandis*, and walnut trees; *ii*) to reconstruct phylogenetic relationship of the new species with other *Bursaphelenchus* species; and *iii*) to develop rapid diagnostics for this species using PCR with species-specific primers.

Materials and methods

Nematode samples

The wood samples with nematodes and beetles were collected from hybrid walnut trees (*J. hindsii* × (*J. nigra* × *J. hindsii*/*J. californica*)), in the Sierra Gold Orchard, Sutter County, California, USA (Fig. 1). Extraction from the bark was done by a modification of the Baermann funnel technique (Ryss, 2017a). Nematodes were also collected in clusters from *P. juglandis* beetles, each dauer being separately attached by the head end to the undersides of the elytra (Fig. 2G, H).

Nematodes were inoculated into cultures of the fungus *Botrytis cinerea* Pers. maintained on 2% potato dextrose agar (PDA) prepared from fresh potatoes and agar (Ryss, 2015). Before nematode inoculation, the fungus was grown for 1 week at room temperature until the white mycelium covered the agar surface. Twenty nematode specimens (females, males and juveniles) were used as the inoculum. Using the mycelium as food, the nematodes increased to thousands of individuals per Petri dish in 3-4 weeks.

Light (LM) and Scanning Electron Microscopy (SEM) studies

Nematode fixation in TAF and slide preparation for LM were done by the express technique (Ryss, 2017b). Morphology of all stages was studied with Nomarski interference contrast using a Leica microscope equipped with a digital camera. Some juveniles, fixed in TAF and processed to anhydrous glycerin, were stained with methylene blue. A 10 μl drop of saturated water solution of methylene blue was added to the drop of suspension of nematode juveniles in glycerin on a 75 × 25 mm slide. After 12 h the stained suspension was covered with a 20 × 20 mm cover slip previously sealed on its edges with a

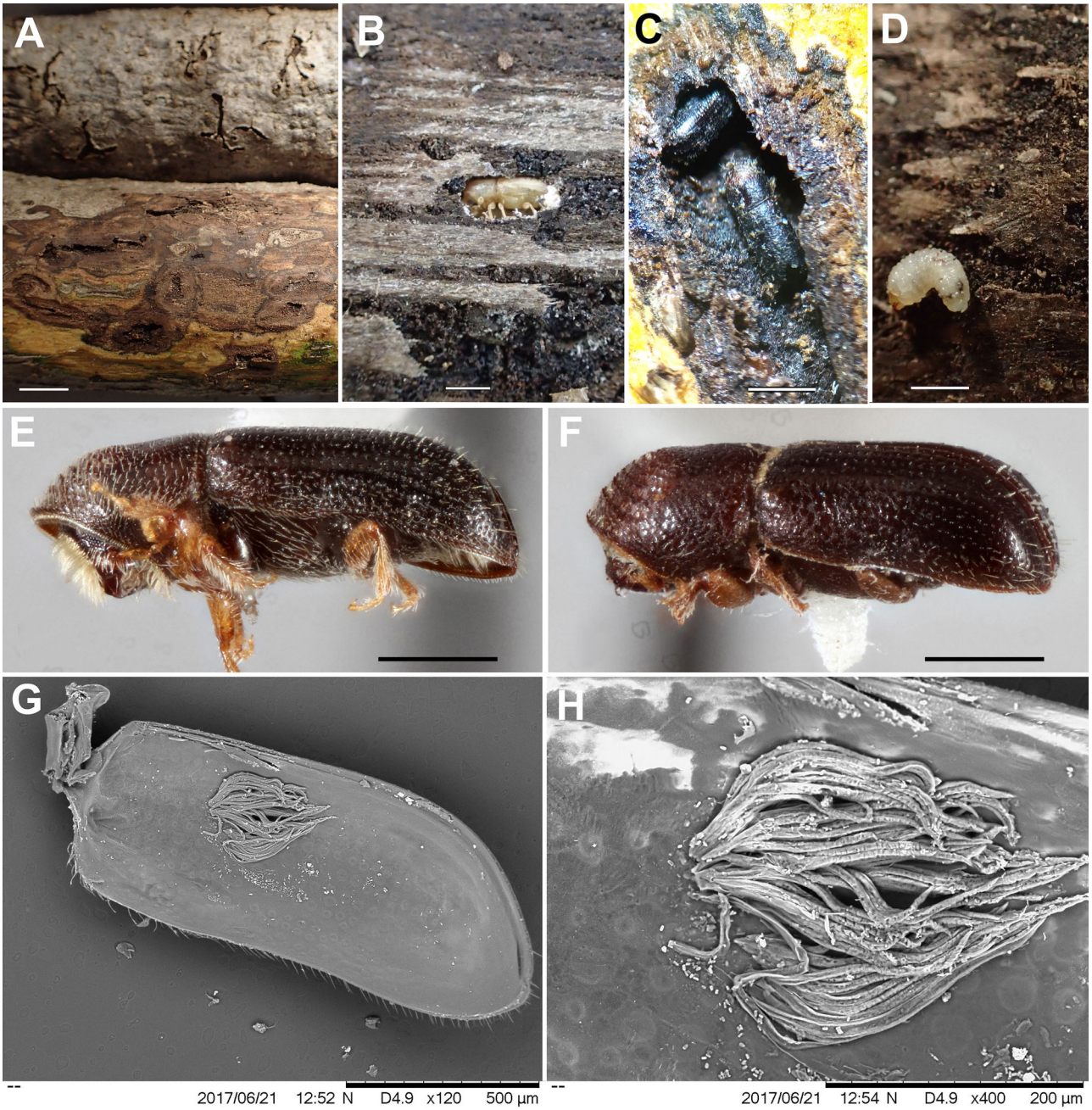

Fig. 2. Vector of the thousand cankers disease: the walnut twig beetle *Pityophthorus juglandis*. A: Branches of *Juglans* sp. (upper: bark with beetle outlets; lower: beetle tunnels); B, C: Beetle imagos in beetle tunnels (B: Light yellow imago in pupal chamber; C: Black imago in nuptial chamber); D: Larval beetle tunnels in branch of *Juglans* sp. with larva of *P. juglandis*; E: Female beetle imago; F: Male beetle imago; G: Excised elytra of *P. juglandis* with *Bursaphelenchus juglandis* n. sp. grouped in clusters with the dauers attached by their anterior ends to the undersides of the elytra (SEM); H: Nematode cluster enlarged (SEM). (Material from California, USA). (Scale bars: A = 10 mm; B-D = 1 mm; E, F = 500 μm.)

thin film of glycerin jelly. After quickly heating at 60°C on a hot plate the drop spread to the edges of the cover slip; thus, the suspension was flattened and fixed with a glycerin jelly frame. The juveniles were studied and photographed under Leica microscope. Following their examination and identification, a few specimens preserved in glycerin were selected for observation under SEM using the protocol of Álvarez-Ortega & Peña-Santiago (2016). The nematodes were hydrated in distilled water, dehydrated in a graded ethanol and acetone series, critical point-dried, coated with gold, and observed with a Zeiss Merlin microscope. Photographs of the beetle elytra with attached nematode clusters were taken using a Hitachi TM3030 tabletop scanning electron microscope. Due to the SEM's low-vacuum functionality, no special preparation was needed for the specimens.

DNA EXTRACTION, PCR, SEQUENCING AND PHYLOGENETIC ANALYSIS

DNA was extracted from several pooled nematodes using proteinase K. PCR and sequencing protocols were as described by Tanha Maafi *et al*. (2003). The primer set: D2A (5′-ACA AGT ACC GTG AGG GAA AGT TG-3′) and D3B (5′-TCG GAA GGA ACC AGC TAC TA-3′) (Subbotin *et al*., 2006) was used for amplification of the D2-D3 expansion segments of 28S rRNA gene. The primer set: G18SU (5′-GCT TGC CTC AAA GAT TAA GCC-3′) and R18Tyl1 (5′-GGT CCA AGA ATT TCA CCT CTC-3′) (Chizhov *et al*., 2006) was used for amplification of the partial 18S rRNA gene. The primer set: 18S (5′-TTG ATT ACG TCC CTG CCC TTT-3′) and 5368 (5′-TTT CAC TCG CCG TTA CTA AGG-3′) (Vrain, 1993) was used for amplification of the ITS rRNA gene. Sequencing was done at Quintara Biosciences. New sequences were deposited in the GenBank under accession numbers: MN759734-MN759736.

The D2-D3 expansion segments of 28S rRNA, 18S rRNA and ITS rRNA gene sequences of *Bursaphelenchus* spp. from GenBank (Ye *et al*., 2007; Pedram *et al*., 2011; Ryss *et al*., 2015; Kanzaki *et al*., 2018; Wang *et al*., 2018a, b; Tomalak & Filipiak, 2019; Gu *et al*., 2019 and others) were included with the new sequences for phylogenetic reconstruction. Outgroup taxa for each dataset were chosen according to previously published data (Ryss *et al*., 2013; Ryss & Subbotin, 2017). The newly obtained and published sequences for each gene were aligned using ClustalX (Thompson *et al*., 1997). ClustalX was run with default (gap opening – 15.0; gap extension – 6.66) parameters for the 18S rRNA dataset and modified (gap opening – 5.0; gap extension – 3.0) parameters for the 28S D2-D3 and ITS rRNA gene datasets. Two ITS rRNA gene sequence alignment were analysed: *i*) full length automatic alignment generated by ClustalX; and *ii*) culled alignment obtained after eliminating poorly aligned segments by Gblocks 0.91b (http://phylogeny.lirmm.fr; Dereeper *et al*., 2008) with default options from a full length automatic alignment. The alignments were analysed with Bayesian inference (BI) using MrBayes 3.1.2 (Ronquist & Huelsenbeck, 2003) using the GTR + I + G model. BI analysis for each gene was initiated with a random starting tree and was run with four chains for 1.0×10^6 or 3.0×10^6 generations. The Markov chains were sampled at intervals of 100 generations. Two runs were performed for each analysis. After discarding burn-in samples and evaluating convergence, the remaining samples were retained for generating a 50% majority-rule consensus tree. Posterior probabilities (PP) are given when they equal or exceed 70%. Other analyses of aligned data were performed with PAUP* 4b10 (Swofford, 2003). Pairwise divergences between taxa were presented as absolute distance values and as percentage mean distance values based on the entire alignment, with adjustment for missing data for each gene.

PCR WITH SPECIES-SPECIFIC PRIMER

Species-specific primer for *B. juglandis* n. sp. was designed using the sequence alignment of the ITS rRNA gene. The PCR mixture was prepared as described by Tanha Maafi *et al*. (2003). The following primer combination was used: forward universal primer F194 (5′-CGT AAC AAG GTA GCT GTA G-3′) (Ferris *et al*., 1993) and species-specific primer ITS-jugR2 (5′-TAT GTT GAA AGA ATG GAC CGC-3′). The PCR amplification profile consisted of 4 min at 94°C; 30 cycles of 1 min at 94°C, 45 s at 57°C and 45 s at 72°C, followed by a final step of 10 min at 72°C. Two μl of the PCR products were separated by electrophoresis on a 1.4% TAE buffered agarose gel, stained and photographed.

Four known *Bursaphelenchus* species were used to test the specificity of the PCR with the newly designed species-specific primer.

Results

Bursaphelenchus juglandis[*] n. sp.
(Figs 3-9)

MEASUREMENTS

See Tables 1-3.

DESCRIPTION

Adults

Body C-shaped after heat relaxation, 0.32-0.71 mm long in specimens from *in vitro* culture. Lateral field with three incisures (two closely adjacent bands). Cephalic region set-off, strongly elevated, hemispherical, its diam. (6-8 μm) twice as wide as high (3-4 μm). At border of cephalic region and body are two annuli: posterior border annulus twice as wide as anterior, but 50% narrower than body annuli. Some folds at base of cephalic region look like fragments of an additional incomplete cephalic annuli. Cephalic region six-lobed: two lateral, two subdorsal and two subventral sectors, each supported by a median cuticular ridge, contour of which is apparent on sector surface. Sectors smooth and devoid of annuli, intersector surface may be folded with annulation but folds are not regular. In addition to these folds between sectors, base of cephalic region is devoid of annulation. Labial region marked with anterior spindle-shaped disc elongated in lateral axis. Disc separated from cephalic region by a groove. Stoma round, in centre of disc. Four pore-like labial sensilla situated in subdorsal and subventral positions on bridge-like radii just opposite to corresponding cephalic sectors. Two lateral labial sensilla pore-like, situated at outer margins of disc, just opposite to lateral head sectors. Paired amphids ring-shaped, with medium-sized pore-like outlets with glandular secretion, situated at borders of lateral sectors close to disc at a distance equal to disc radius. Four papilliform cephalic sensilla, situated at subdorsal and subventral sectors at same distance as amphids from disc, thus forming outer circle of cephalic sensory structures. Each cephalic sensilla slightly shifted to lateral direction from mid-line of its sector surface. Mid-line marked by cuticular ridge, each subdorsal sensilla shifted ventrally from ridge, subventral sensilla shifted slightly dorsally from median ridge of sector. Cephalic sensory structures may be expressed by formula: six labial sensilla (two lateral + four sublateral); four cephalic sensilla, two amphids. Stylet 11-13 μm long with three knob-like basal thickenings, conical part 40% of its length, inner lumen wide, its inner diam. is equal to wall thickness. Median bulb oval, 13-14 $\times$ 10-11 μm in size, its length 1.1-1.5 times longer than diam., sometimes rounded, muscular, with a central valve. Pharyngo-intestinal junction a muscular sphincter with an inner small pyriform valve. Nerve ring 40-65 μm from anterior body end, encircling intestine posterior to pharyngo-intestinal junction. Excretory pore distinct, 41-65 μm from anterior body end, mostly at base of median bulb or at its centre, or shifted to anterior border of median bulb. Hemizonid 3-5 annules wide, posterior to median bulb for twice its diam. Pharyngeal glands in a lobe 44-130 μm long overlapping mid-intestine dorsally, 4-7 body diam. at median bulb long, posterior nucleus of gland lobe twice diam. of two anterior ones, large posterior nucleus belongs to dorsal gland, two small anterior nuclei situated in bodies of subventral glands.

Male

Testis situated to right side of intestine, its distal ending reflexed ventrally at mid-body, spermatocytes in multiple rows, spermatid zone a quartet of large round cells at middle of genital tube, anterior to this zone spermatocytes form a mass of nuclei, posteriorly, immature sperm cells are polygonal with distinct individual cell borders. In last third of testis sperm cells are spherical, each spermatozoon with vesiculated cytoplasmic sphere around compact nucleus, thick-walled lumen containing secretory granules, opening in cloacal sac near rectum. Cloacal sac with paired separate spicules. Spicule 10-12 μm long, widened, 1.7-2.3 as long as capitulum width and 3.1-4.6 as long as spicule width posterior to rostrum. Condylus bluntly rounded, curved dorsally, rostrum angular to conically rounded, outer lateral side of spicule with two incisures: wide 'median piece'[*] continuing from capitulum centre to tip, dorsal incisure narrow, starting posterior to rostrum. Tip conically rounded bearing small cucullus. Spicule dorsally angular, two virtual lines: *i*) condylus-rostrum; and *ii*) line extending spicule ending from dorsal side of blade, almost parallel. Caudal papillae: P1, P2, P3, GP (P5); P1 (unpaired) papilliform, 1-2 μm anterior to cloacal opening. P2 paired papilliform at same level as P1 but at lateral borders of cloacal opening, P3 paired

[*] The specific epithet is formed from *Juglans*, the Latin name of the plant host genus.

[*] The term 'median piece' was proposed by Peña-Santiago *et al.* (2014) for the spicules of dorylaimid nematodes. The structure in aphelenchoidids is homologous to that of dorylaims.

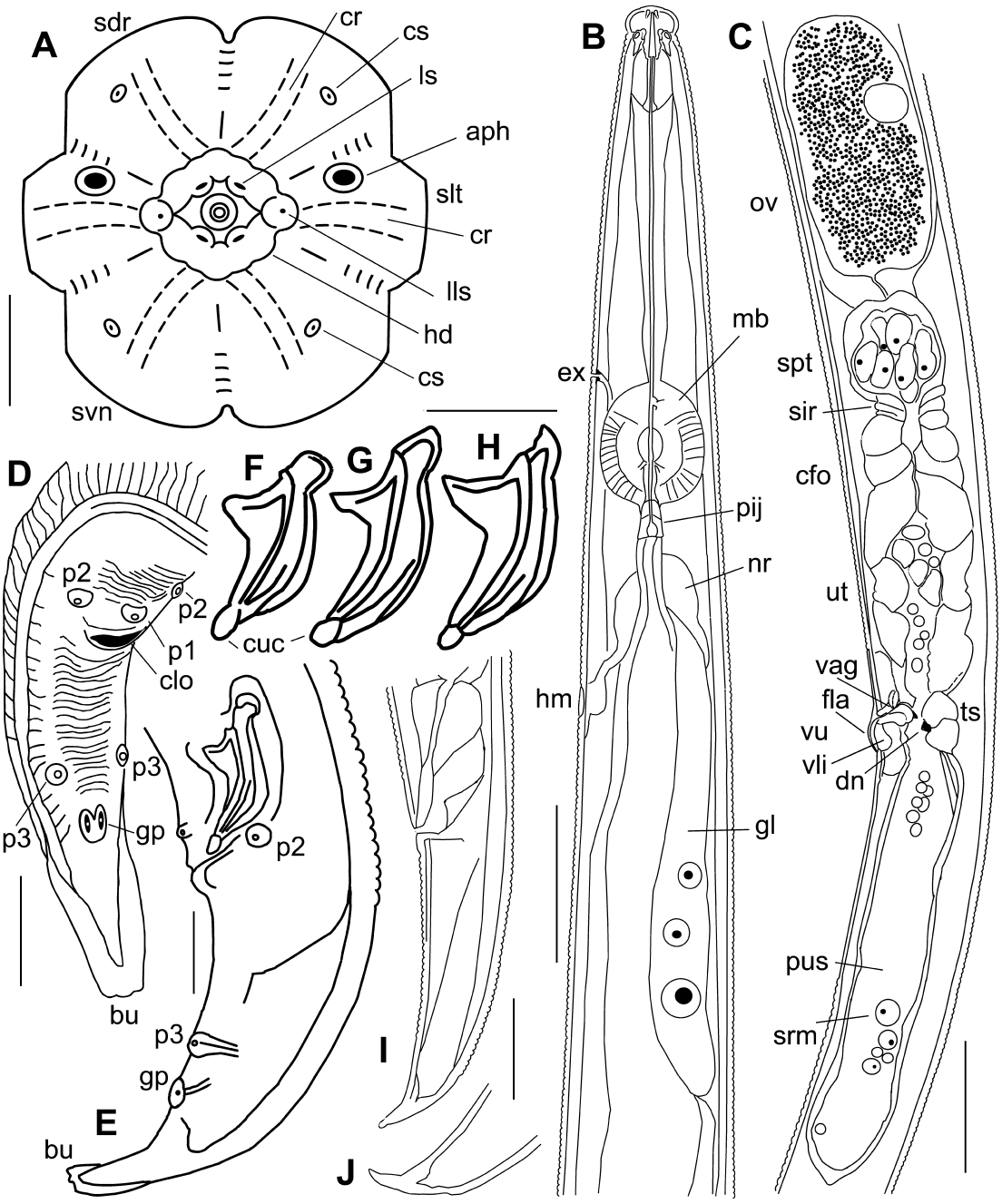

Fig. 3. *Bursaphelenchus juglandis* n. sp. A: Male cephalic region, *en face* view (aph = amphid, cr = cephalic ridge, cs = cephalic sensilla, hd = cephalic disc, lls = lateral sensillum, ls = labial sensillum, sdr = subdorsal head sector, slt = sublateral head sector, svn = subventral head sector); B: Anterior body of female (ex = excretory pore, gl = pharyngeal gland lobe, hm = hemizonid, mb = median bulb, nr = nerve ring, pij = pharyngo-intestinal junction); C: Female genital system (part) (cfo = crustaformeria, dn = vaginal denticles, fla = vulval flap, ov = ovocyte in proximal part of ovary, pus = post-vulval uterine sac, sir = sphincter of spermatheca, spt = spermatheca, srm = sperm cell, ts = two = celled structures, ut = anterior uterus, vag = vagina, vli = posterior vulval lip, vu = vulva); D, E: Male tail with caudal papillae (D: Ventral view, E: Lateral view (clo = cloacal opening, gp = gland papilla on plate, p1-p3 = caudal papillae, bu = bursal flap)); F-H: Male spicules (cuc = cucullus); I: Female tail. J: Female tail tip. A, D: Drawings from SEM photographs. (Scale bars: A = 1 μm; B, C = 20 μm; D-H = 5 μm; I, J = 10 μm.)

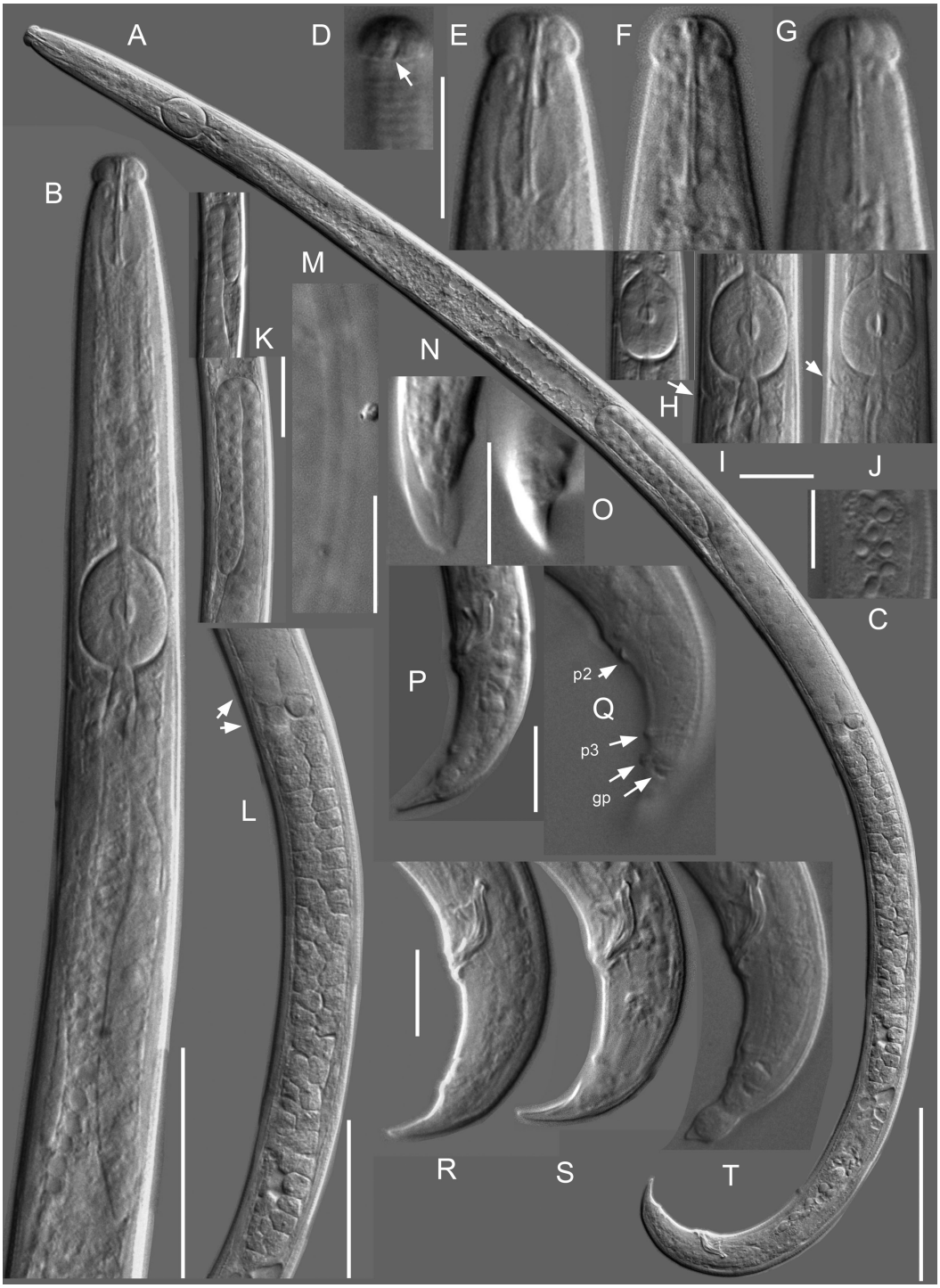

Fig. 4. *Bursaphelenchus juglandis* n. sp. Male. A: General outline; B: Anterior body; C: Sperm cells; D: Head surface with amphid (arrow); E-G: Head with stylet; H-J: Median bulb and excretory pore (arrows); K: Anterior ends of testis; L: Testis, central part with spermatid zone (arrows); M: Lateral field; N: Bursa, ventral view; O: Bursa, lateral view with gland papillae; P, Q: Male tail with paired papilliform papillae (p2, p3) and genital papillae (gp); R-T: Male tail with spicules. (Scale bars: A = 50 μm; B = 30 μm; C-J, N-T = 10 μm; K, L = 20 μm; M = 30 μm.)

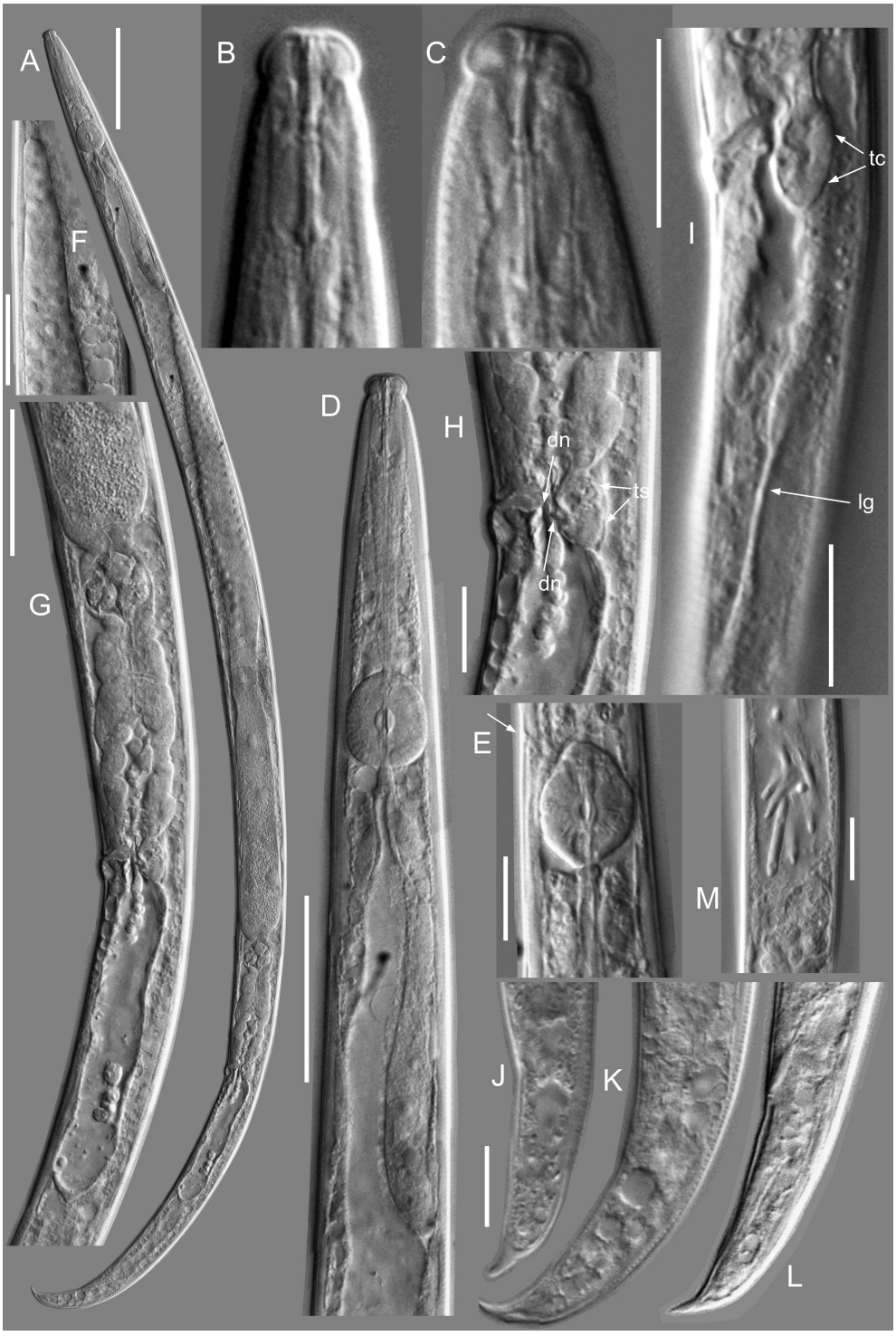

Fig. 5. *Bursaphelenchus juglandis* n. sp. Female. A: General outline; B, C: Head with stylet. D: Anterior body; E: Median bulb and excretory pore (arrow); F: Anterior end of ovary; G: Vulva, spermatheca, crustaformeria and uterus; H: Vulval region showing denticles (dn) and two-celled structures (ts) in uterus junction; I: Vulval region with a ligament (lg) along posterior uterus; J-L: Tail, lateral view; M: Gregarine parasites in mid-intestine. (Scale bars: A = 50 μm; B, C, E, H-M = 10 μm; D, G = 30 μm; F = 20 μm.)

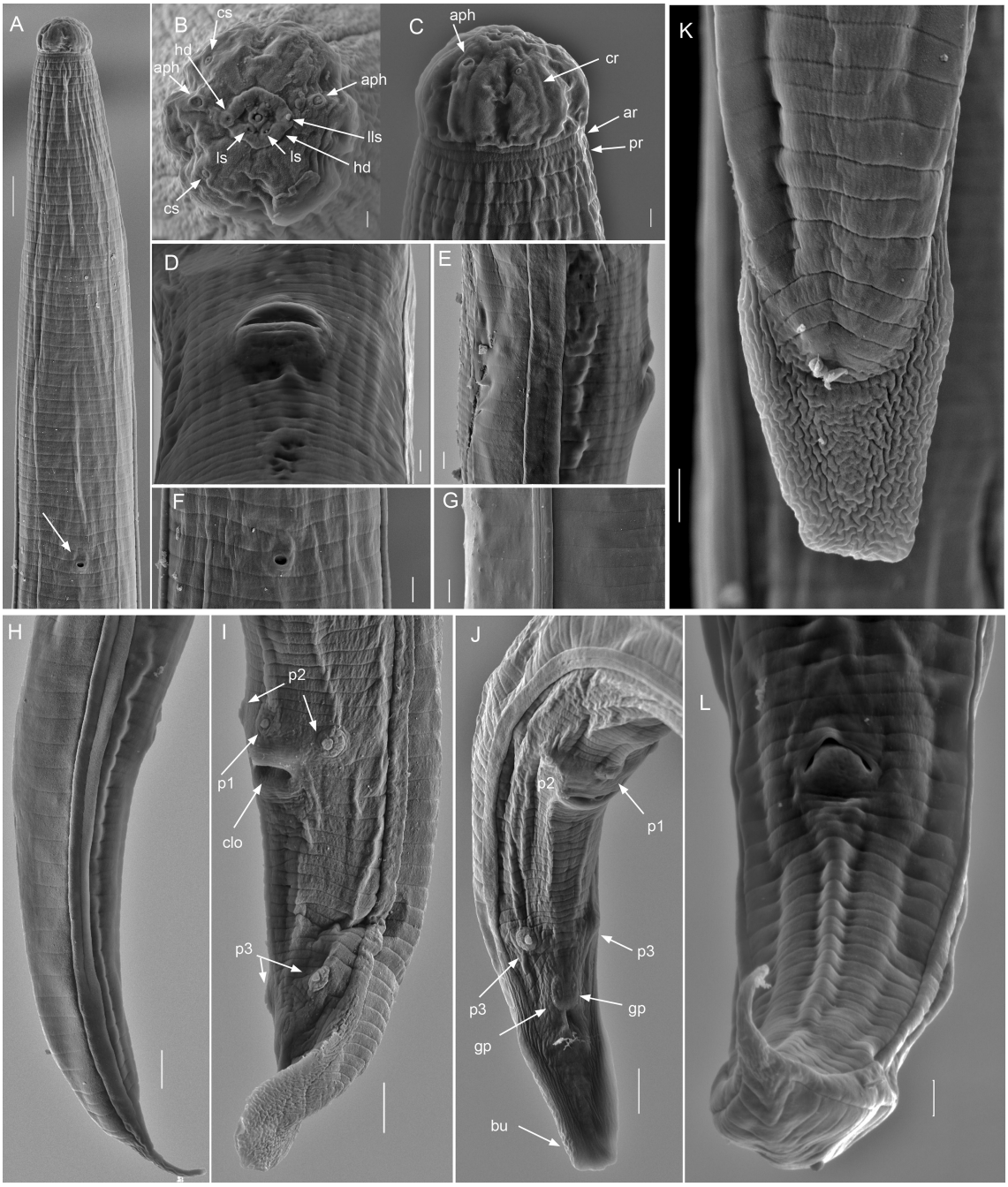

Fig. 6. *Bursaphelenchus juglandis* n. sp. SEM photographs. A: Male anterior with excretory pore (arrow), ventral view; B: Male cephalic region *en face* view with sensilla (aph = amphid; cs = cephalic sensilla; hd = cephalic disc; ls = labial sensilla; lls = lateral labial sensillum); C: Male head lateral view (aph = amphid; ar = anterior border annulus; cr = cephalic ridge; pr = posterior border annulus); D: Vulva, ventral view; E: Vulva, lateral view with lateral field; F: Male excretory pore, ventral view; G: Male lateral field; H: Female tail, lateral view; I, J: Male tail with caudal papilla, ventral view (bu = bursa; clo = cloacal opening; gp = gland papillae (P5); p1, p2, p3 = papilliform papillae); K: Male bursa, dorsal view; L: Female tail, ventral view. (Scale bars: A = 3 μm; B = 300 nm; C = 400 nm; D-G = 1 μm; H-J = 2 μm; K, L = 1 μm.)

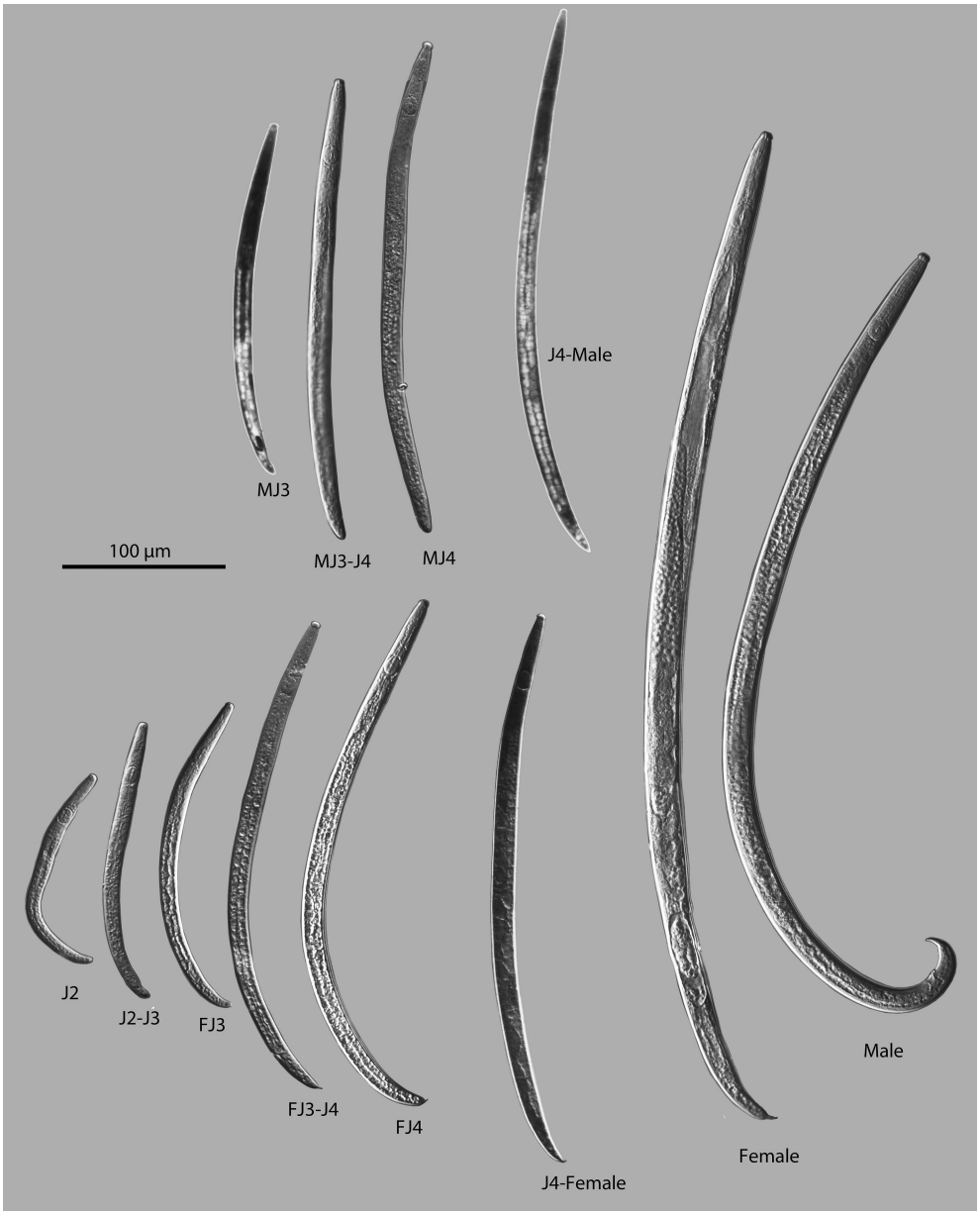

Fig. 7. Male and female development stages of *Bursaphelenchus juglandis* n. sp. Second-, third- and fourth-stage juveniles = J2, J3, J4, respectively; F = female; M = male; moulting individuals are indicated by a hyphen linking stages, *e.g.*, J3-J4.

papilliform at 40-53% of tail length; P5 are paired gland papillae (GP) elongated slit-like pores, just anterior to bursal flap, contiguous to each other, situated on elongated heart-like bi-oval plate on ventral midline, 52-69% of tail length. A pair of the P4 papilliform caudal papillae absent. Bursa 4-7 μm along midline, oval, scoop-shaped, its ending blunt or slightly trident-like.

Female

Female genital system monoprodelphic, consisting of fully developed and functional anterior branch and posterior branch including an undifferentiated post-uterine sac. Anterior branch including ovary, oviduct, spermatheca, crustaformeria, anterior uterus, vagina and vulva. Ovary

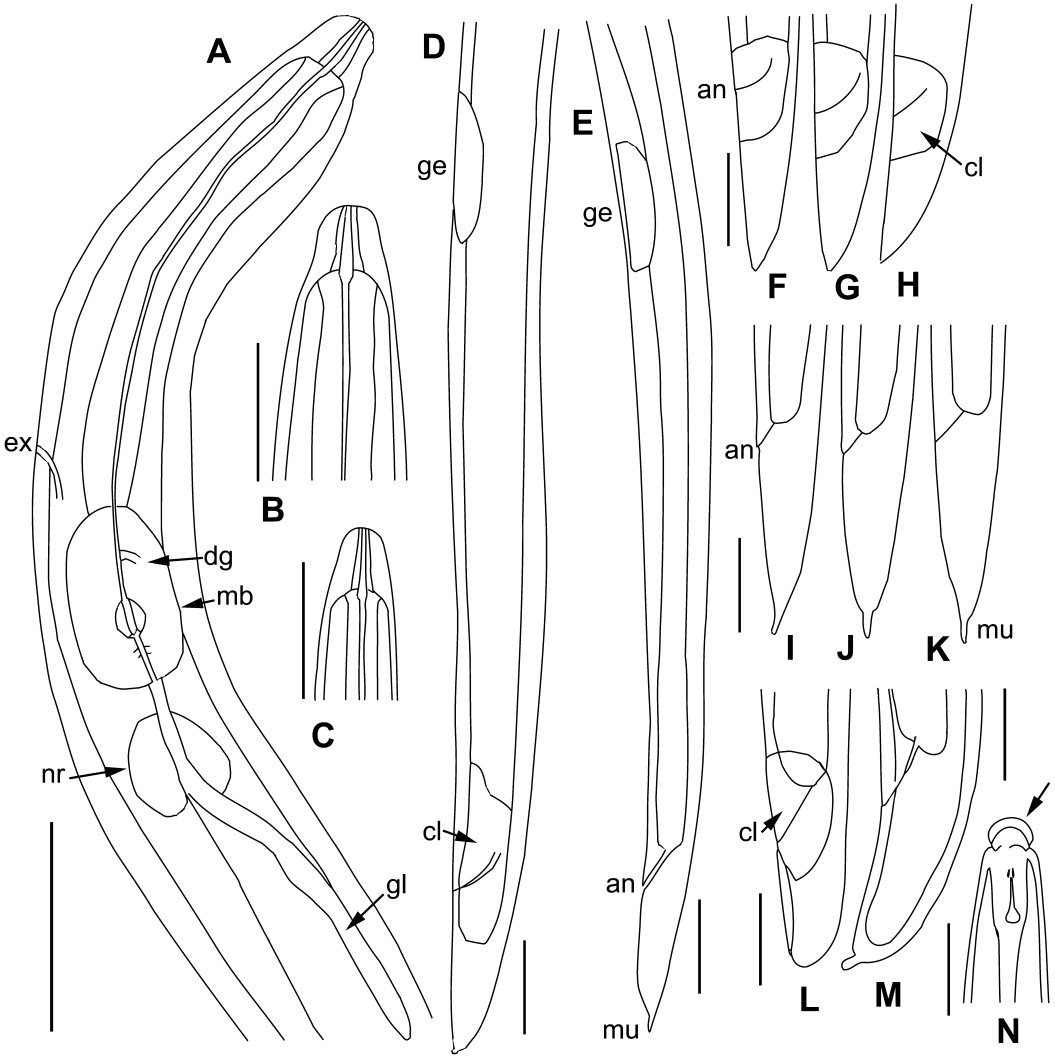

Fig. 8. Dauer juveniles (DJ3) and fourth-stage juveniles (J4) of propagative generation. A: Anterior end of DJ3 (dg = dorsal pharyngeal gland duct opening in anterior part of median bulb; ex = excretory pore; gl = pharyngeal gland lobe; mb = median bulb; nr = nerve ring); B, C: Cephalic region of DJ3; D: Posterior part of male DJ3 (cl = cloacal primordium; ge = genital primordium); E: Posterior part of female DJ3 (an = anus; ge = genital primordium; mu = mucron at tail tip); F-H: Tail shape of male dauer (an = anus; cl = cloacal primordium); I-K: Tail shape of female dauer; L: Blunt tail tip shape of J4 male juvenile of propagative generation (cl = cloacal primordium); M: Mucronate tail tip of female juvenile J4 of the propagative generation; N: Shed cephalic cuticle during moult from J3 to J4 female juvenile (arrow). (Scale bars = 10 μm.)

in cultured specimens on right side from mid-intestine, its end reaching pharyngeal gland lobe, straight conical. Anterior (distal) part of ovary conical with numerous nuclei of oocytes in 5-6 rows, proximal expanded part forming a single row of oocytes, 2-3 posteriormost oocytes enlarged and granulated. Spermatheca a blind sac 16 $\times$ 12 μm in size, situated on right side of ovary, slightly oval to spherical (length: width ratio 1:2), sometimes distinctly bilobed, with inner cavity filled with amoeboid oval sperm 3-4 $\times$ 6-7 μm in size, with a voluminous vesiculated cytoplasmic part and small nucleus. At base of spermatheca a small muscular sphincter surrounding narrow duct between spermatheca and crustaformeria. Oviduct and spermatheca opening into crustaformeria, which is connected with short anterior uterus, length of which is equal to crustaformeria. Anterior uterus consisting of polygonal

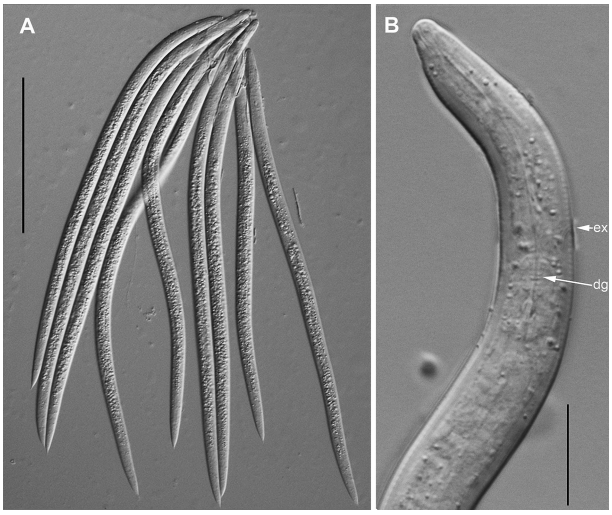

Fig. 9. Dauer juveniles (DJ3). A: Agglomeration of DJ3 under elytra of beetle imago; B: Anterior end of DJ3 (dg = dorsal pharyngeal gland duct opening in anterior part of median bulb; ex = excretory pore). (Scale bars: A = 100 μm; B = 10 μm.)

cells with thick-walled lumen filled with mucous secretion. Vulva bordered anteriorly by arched flap with 4-6 μm lateral flanges, its opening transverse, devoid of papillae. Vulval posterior lip enlarged, swollen. Vagina short, inclined anteriorly and surrounded by a pyriform muscle sphincter. Opposite to vagina a pair of two-celled dense striated structures 7-12 μm long surrounding junction between anterior and posterior parts of uterus. Ventral and dorsal denticles distinct on walls of this junction thus forming 'lock-like' structure between anterior and posterior parts of uterus. Post-vulval uterine sac (PUS) a thin-walled 44-79 μm sac occupying 47-70% of vulva-anus distance or 3.3-4.1 vulval body diam. long, its lumen broad and filled with several sperm cells. PUS situated on left side of mid-intestine, along its lateral sides paired ligaments present connecting junction of two parts of uterus and ventral side of body wall. Rectum a distinct cuticular tube opening ventrally in a slit-like inverted-U-shaped anus. Tail curved ventrally, its hyaline tip hook-like digitate, in many specimens a ventrally curved 3-5 μm mucron visible as a continuation of tail tip.

Juveniles

Juveniles are similar to adult specimens in general characters with exception of genital primordia. First moult to second-stage juvenile (J2) taking place within egg. There are three juvenile stages (J2, J3, J4), divided by two moults (J2-J3 and J3-J4) plus an additional moult, J4-adult. J2-J4 differ in body length, length of genital primordia, ratios of genital primordium to body length, and length of genital primordium to its diam. Moulting individuals (Table 3) may be distinguished by the shed cuticle at cephalic and tail ends and slightly blurry outlines of inner structures. J2 have a strongly ventrally curved body shape *vs* straighter bodies in J3. In non-stained individuals, sexes of juveniles may be easily distinguished at J4. Female J4 has distinct mucronate tail tip, curved ventrally, tail without cloacal primordium, body distinctly C-shaped *vs* male J4 has rounded thick tail without mucron, with distinct dense cloacal primordium, body almost straight. In J3, tails of female and male juveniles are round and devoid of mucron. Cloacal primordium in male juveniles is present (*vs* absent in female J3); however, distinct differences between male and female J3 may be evaluated only in methylene blue stained individuals.

All nematodes described above were initially collected from bark and wood and then multiplied in agar cultures with *B. cinerea*. Additionally, transmission dauer juveniles (DJ3) were collected from undersides of elytra of *P. juglandis*.

Dauer juveniles

Body almost straight, narrow, annulated, with three lines in lateral fields. Head smooth, hemispherical, continuous with body, its height 0.6-0.7 times head diam. Head framework absent, substituted by an inner hyaline cap. Amphidial ducts filled with secretion, continuing posterior for seven head diam. Stylet 6-8 μm, consisting of two parts: anterior part comprising 40% of stylet length with a thin lumen and continuous with stoma; posterior part moderately thick walled, devoid of basal knobs or thickenings. Excretory pore 26-30 μm from anterior end, situated anteriorly to elongated pyriform median bulb. Median bulb consisting of two parts, a spherical basal part and cupola-like anterior part. Spherical part with well-developed cuticular valve in centre and ducts of pharyngeal subventral glands opening posterior to valve. Dorsal pharyngeal gland duct opening midway between valve and anterior edge of bulb. Nerve ring one stylet length posterior to median bulb, surrounding pharyngo-intestinal junction. Pharyngeal gland lobe very thin, 3-6 body diam. long at median bulb, located dorsally. Genital primordium located in posterior body half, at 60-70% of body section between median bulb and anus. Primordium shape different in male and female dauers: in male DJ3 its posterior end slightly expanded *vs* cylindrical in female DJ3. Tail 2.5-4.0 anal body diam. long, conical. Tail tip different between male and female dauers: female DJ3 with distinctly set-off axial mucron of 3 μm, male DJ3 devoid of mucron,

Table 1. Morphometrics of type specimens of *Bursaphelenchus juglandis* n. sp. All measurements are in μm and in the form: mean ± s.d. (range).

Character	Male		Female
	Holotype	Paratypes	Paratypes
n	–	25	25
L	545	505 ± 75 (324-604)	563 ± 94 (432-712)
a	34.1	33.3 ± 3.0 (28.5-38.3)	31.7 ± 4.0 (25.2-37.0)
b	9.1	9.3 ± 1.3 (7.0-12.2)	8.8 ± 1.3 (6.9-11.0)
b′	4.4	3.9 ± 0.5 (3.1-4.6)	4.1 ± 0.6 (3.4-5.5)
c	18.4	18.8 ± 2.2 (15.7-25.9)	18.8 ± 2.6 (15.7-22.8)
c′	2.5	2.6 ± 0.4 (2.0-3.2)	3.3 ± 0.4 (2.6-4.0)
V or T	57.0	58.0 ± 5 (44-65)	75.0 ± 1 (72-77)
Stylet	12.5	12.0 ± 1 (10.5-13.0)	12.0 ± 1 (11.0-13.0)
Cephalic region diam.	7.0	5.9 ± 0.9 (5.0-8.0)	6.5 ± 0.6 (6.0-8.0)
Cephalic region height	3.5	2.8 ± 0.4 (2.5-3.5)	3.2 ± 0.4 (2.5-4.0)
Median bulb length (MBL)	14.0	12.0 ± 1 (9.0-15.0)	14.0 ± 2 (12.0-16.0)
Median bulb diam. (MBD)	11.0	9.0 ± 1 (7.0-11.0)	11 ± 2 (8.0-14.0)
MBL/MBD	1.3	1.3 ± 0.1 (1.1-1.7)	1.3 ± 0.1 (1.1-1.5)
Excretory pore from anterior	62	53 ± 9 (41-62)	53 ± 7 (45-65)
Nerve ring posterior border, from anterior	74	70 ± 7 (58-80)	75 ± 8 (66-86)
Pharynx	60	54 ± 6 (41-62)	64 ± 8 (49-75)
Anterior to pharyngeal gland lobe end	125	131 ± 19 (102-179)	140 ± 23 (93-178)
Pharyngeal gland lobe	65	76 ± 21 (54-130)	76 ± 18 (44-112)
Pharyngeal gland lobe/body diam.	4.6	6.4 ± 1.9 (4.2-10.6)	5.4 ± 0.9 (3.6-6.8)
Max. body diam.	16.0	15.0 ± 2 (11.0-19.0)	18.0 ± 2 (13.0-20.0)
Vulva-anus distance	–	–	110 ± 20 (89-147)
Posterior genital branch	–	–	66 ± 15 (44-110)
Posterior genital branch/vulval body diam.	–	–	3.7 ± 0.7 (2.9-5.8)
Posterior genital branch/vulva-anus distance (%)	–	–	60 ± 9 (47-80)
Tail	30	27 ± 4.0 (18-33)	30 ± 5.0 (23-40)
Anal body diam.	12	10 ± 1.0 (8-13)	9 ± 1.0 (8-11)
Annuli (width of 10 at mid-body)	8.3	7.6 ± 1.4 (6.3-9.8)	7.4 ± 0.4 (7.0-8.0)
Spicule length (arc)	11.5	11.0 ± 0.9 (9.5-12.0)	–
Capitulum width	6.5	5.9 ± 0.7 (5.0-6.8)	–
Spicule length/capitulum length	1.8	1.9 ± 0.2 (1.7-2.3)	–
Spicule L/W	4.2	3.9 ± 0.5 (3.1-4.6)	–
Anus-P3/tail length	40	45 ± 5 (40-53)	–
Anus-P5/tail length	52	59 ± 6 (52-69)	–
Bursa to lateral wings	10	9 ± 2 (5-12)	–
Bursa midline	7	5 ± 1 (4-7)	–

tail tip slightly ventrally curved, conical, at anus expanded cloacal primordium distinct on dorsal side of rectum.

NOTE

The DJ3 are located under the elytra of beetle imagos. They represent a significantly modified juvenile stage aimed both at overwintering and transmission to healthy trees. Dauers are attributed to the J3 stage because of their similarities with the J3 of the propagative juveniles in body length, genital primordium size, and values of the indices: a, b, b′ c, c′. Clusters of 10-30 DJ3 are located in groups under the beetle elytra with their heads at the base of the elytra. Dauers are immotile until placed in a water drop when they start to move in 20-30 min and over 2 h begin to moult forming the J4 that are morphologically similar to the J4 of the propagative stage.

Table 2. Morphometrics of the development stages (second-stage juvenile = J2; third-stage juvenile = J3; fourth-stage juvenile = J4; third-stage dauer = DJ3) of *Bursaphelenchus juglandis* n. sp. All measurements are in μm and in the form: mean ± s.d. (range).

Character	J2	J3 male	J3 female	DJ3	J4 male	J4 female
n	40	15	20	10	20	40
L	163 ± 16 (134-203)	194 ± 15 (176-220)	194 ± 14 (176-227)	295 ± 37 (210-330)	314 ± 20 (283-347)	329 ± 19 (295-357)
a	19.3 ± 2.2 (15.2-23.7)	18.4 ± 1.5 (16.5-21.4)	20.2 ± 2.2 (17.5-24.1)	28.1 ± 2.5 (23.2-31.3)	24.9 ± 2.3 (21.7-31.3)	26.8 ± 3.5 (20.7-34.2)
b	4.8 ± 0.6 (4.1-6.1)	4.8 ± 0.3 (4.5-5.4)	5.0 ± 0.6 (4.3-6.3)	7.2 ± 0.8 (5.5-8.0)	6.8 ± 0.5 (6.0-8.0)	6.6 ± 0.4 (5.6-7.2)
b′	2.4 ± 0.3 (1.7-2.8)	2.1 ± 0.2 (1.8-2.4)	2.2 ± 0.3 (1.8-2.8)	3.9 ± 0.5 (2.6-4.4)	3.0 ± 0.4 (2.5-3.6)	2.8 ± 0.3 (2.2-3.7)
c	14.4 ± 2.2 (10.5-20.5)	13.5 ± 0.4 (12.7-13.9)	14.6 ± 1.8 (12.4-18.4)	14.2 ± 1.4 (11.6-15.8)	16.4 ± 3.6 (12.8-22.6)	13.6 ± 2.1 (10.6-20.8)
c′	2.3 ± 0.4 (1.7-3.1)	2.3 ± 0.2 (2.0-2.7)	2.4 ± 0.2 (2.0-2.7)	3.2 ± 0.4 (2.6-3.9)	2.3 ± 0.6 (1.4-3.0)	3.1 ± 0.5 (1.9-4.1)
Body diam.	9 ± 1(7-11)	11 ± 1 (9-12)	10 ± 1 (8-11)	11 ± 1 (8-11)	13 ± 1 (9-15)	12 ± 1 (10-15)
Pharynx	34 ± 3 (29-40)	41 ± 2 (38-43)	39 ± 3 (33-43)	41 ± 2 (37-43)	47 ± 5 (37-53)	50 ± 3 (44-58)
Pharyngeal gland	36 ± 9 (23-54)	51 ± 6 (45-62)	50 ± 6 (44-62)	34 ± 4 (30-43)	58 ± 11 (44-76)	69 ± 13 (45-93)
Pharyngeal gland/metacorpus body diam.	4.4 ± 1.0 (2.7-7.0)	5.6 ± 0.7 (4.5-6.5)	5.6 ± 0.8 (4.5-6.6)	4.1 ± 0.7 (3.3-5.8)	6.0 ± 1.0 (3.9-7.3)	7.2 ± 1.8 (4.2-12.0)
Stylet	9.4 ± 1.1 (7.5-11)	9.6 ± 0.2 (9.5-10.0)	9.2 ± 0.8 (8-10)	7.4 ± 0.6 (6.5-8.0)	10.7 ± 0.5 (10-12)	10.5 ± 0.8 (9.5-12.0)
Labial region diam.	5.0 ± 0.5 (4.0-6.0)	5.1 ± 0.2 (4.5-5.5)	4.8 ± 0.8 (4.0-6.5)	3.8 ± 0.6 (3.0-4.5)	5.2 ± 0.3 (4.5-6.0)	5.3 ± 0.8 (4.0-6.5)
Labial region height	2.8 ± 0.4 (2.5-3.5)	2.7 ± 0.3 (2.5-3.0)	2.6 ± 0.4 (2.0-3.0)	2.2 ± 0.4 (1.5-3.0)	2.7 ± 0.3 (2.5-3.5)	2.9 ± 0.4 (2.5-4.0)
Median bulb length	9.4 ± 0.6 (8.5-10.5)	9.9 ± 0.5 (9.0-10.5)	9.5 ± 1.5 (7.0-11.5)	10.3 ± 0.8 (9.0-11.5)	10.6 ± 0.8 (9.0-11.5)	11.6 ± 1.4 (9.0-14.0)
Median bulb diam.	7.4 ± 0.7 (6.0-9.0)	7.2 ± 0.6 (6.5-8.0)	6.9 ± 0.6 (6.0-8.0)	6.0 ± 0.3 (5.0-6.5)	7.9 ± 0.8 (6.5-9.5)	8.4 ± 0.9 (6.5-10.0)
Nerve ring from anterior	43 ± 4 (37-50)	50 ± 5 (43-57)	50 ± 5 (44-57)	42.9 ± 2.6 (38.0-46.5)	59 ± 7 (48-68)	62 ± 4 (52-70)
Tail	11.4 ± 1.3 (9.5-14.0)	14.4 ± 1.4 (13.0-16.5)	13.4 ± 1.5 (10.0-16.5)	21.0 ± 3.0 (15.0-25.0)	19.8 ± 3.7 (14.0-24.5)	24.5 ± 3.0 (16.0-28.5)
Anal body diam.	5.1 ± 0.6 (4.0-6.0)	6.3 ± 0.9 (5.0-8.0)	5.6 ± 0.6 (4.5-6.5)	6.5 ± 0.5 (5.5-7.0)	8.7 ± 0.8 (7.5-10.0)	8.0 ± 0.8 (6.5-9.5)
Genital primordium length (GPL)	5.9 ± 1.0 (4.5-7.5)	15.1 ± 4.6 (10.0-23.0)	12.9 ± 2.2 (10.0-16.5)	13.7 ± 1.9 (10.5-16.5)	73 ± 53 (27-150)	51 ± 8 (31-74)
Genital primordium width (GPW)	4.0 ± 0.3 (3.0-4.5)	4.0 ± 0.9 (2.5-5.5)	3.4 ± 0.6 (2.5-4.0)	3.7 ± 0.5 (2.5-4.5)	5.4 ± 0.9 (4.0-6.5)	5.2 ± 0.8 (4.0-7.5)
GPL/GPW	1.5 ± 0.3 (1.1-2.2)	4.0 ± 1.5 (2.4-6.0)	4.0 ± 1.3 (2.6-6.0)	3.8 ± 0.6 (3.1-4.6)	13.6 ± 9.2 (4.2-30.4)	10.1 ± 2.3 (6.0-16.9)
GPL/L. %	4 ± 1 (3-5)	8 ± 3 (5-13)	7 ± 1 (5-9)	4.7 ± 0.7 (3.5-5.9)	24 ± 8 (8-48)	16 ± 3 (9-21)
Labial region diam./height	1.8 ± 0.3 (1.5-2.4)	1.9 ± 0.1 (1.8-2.1)	1.8 ± 0.2 (1.7-2.1)	1.7 ± 0.1 (1.5-1.8)	1.9 ± 0.2 (1.6-2.3)	1.9 ± 0.2 (1.4-2.3)
Median bulb length/width	1.3 ± 0.1 (1.1-1.5)	1.4 ± 0.1 (1.3-1.5)	1.4 ± 0.1 (1.2-1.6)	1.7 ± 0.1 (1.6-1.9)	1.4 ± 0.1 (1.1-1.6)	1.4 ± 0.2 (1.2-1.9)

Table 3. Morphometrics of the moulting development stages (second-stage juvenile = J2; third-stage juvenile = J3; fourth-stage juvenile = J4) of *Bursaphelenchus juglandis* n. sp. All measurements are in μm and in the form: mean ± s.d. (range).

Character	Moult J2-J3	Moult J3-J4 male	Moult J3-J4 female	Moult J4-male	Moult J4 female
n	5	3	3	4	4
L	182 ± 15 (164-199)	243 ± 58 (201-284)	310 ± 2 (308-311)	407 ± 60 (348-468)	371 ± 41 (346-432)
a	20.4 ± 2.6 (18.3-23.9)	19.1 ± 1.4 (18.1-20.1)	25.2 ± 1.1 (24.4-26.0)	27.1 ± 4.1 (23.3-31.5)	26.9 ± 4.6 (21.7-32.7)
b	4.5 ± 0.3 (4.3-5.0)	5.2 ± 0.4 (4.9-5.5)	6.6 ± 0.1 (6.5-6.6)	8.2 ± 0.5 (7.7-8.7)	7.4 ± 0.6 (7.0-8.3)
b′	2.1 ± 0.2 (1.7-2.3)	2.4 ± 0.1 (2.3-2.5)	3.0 ± 0.1 (3.0-3.1)	3.4 ± 0.7 (2.6-3.8)	3.1 ± 0.4 (2.8-3.7)
c	12.9 ± 2.2 (10.3-15.1)	15.0 ± 4.1 (12.2-17.9)	14.1 ± 0.4 (13.8-14.4)	14.8 ± 0.9 (14.2-15.8)	15.3 ± 2.3 (13.5-18.5)
c′	2.9 ± 1.1 (2.1-4.6)	2.0 ± 0.4 (1.7-2.3)	2.9 ± 0.4 (2.6-3.1)	2.4 ± 0.1 (2.4-2.5)	2.9 ± 0.4 (2.6-3.4)
Body diam.	9 ± 1 (8-10)	13 ± 2 (11-14)	12 ± 1 (12-13)	15 ± 1 (14-16)	14 ± 1 (13-16)
Pharynx	40 ± 2 (37-42)	46 ± 8 (41-52)	47 ± 1 (47-48)	50 ± 7 (42-54)	50 ± 3 (46-52)
Pharyngeal gland	49 ± 9 (36-62)	54 ± 11 (46-61)	55 ± 3 (53-56)	71 ± 18 (54-90)	69 ± 9 (58-79)
Pharyngeal gland/metacorpus body diam.	5.8 ± 1.2 (3.9-7.1)	5.3 ± 0.1 (5.2-5.4)	5.2 ± 0.3 (5.0-5.4)	6.4 ± 2.6 (4.6-9.4)	6.5 ± 1.7 (4.7-8.7)
Stylet	8.4 ± 0.7 (8.0-9.5)	9.5 ± 0.1 (9.0-10.0)	10.7 ± 1.3 (9.5-11.5)	11.9 ± 0.7 (11.5-12.5)	12.1 ± 1.4 (11.0-14.0)
Labial region diam.	4.7 ± 0.1 (4.5-5.0)	5.8 ± 0.4 (5.5-6.0)	5.3 ± 0.4 (5.0-5.5)	6.4 ± 0.9 (5.5-7.0)	5.6 ± 0.4 (5.0-6.0)
Labial region height	3.1 ± 0.1 (3.0-3.5)	3.1 ± 0.1 (3.1-3.2)	3.0	3.3 ± 0.8 (2.5-4.0)	2.0 ± 0.1 (2.0-2.5)
Median bulb length	9.6 ± 1.1 (8.0-11.0)	11.2 ± 0.4 (11.0-11.5)	10.8 ± 0.1 (10.5-11)	12.5 ± 1.1 (11.5-13.5)	13.0 ± 0.4 (12.5-13.5)
Median bulb diam.	6.9 ± 0.7 (6.0-8.0)	7.6 ± 2.7 (5.5-9.5)	9.1 ± 0.4 (8.5-9.5)	8.7 ± 0.4 (8.5-9.0)	8.6 ± 0.6 (8.0-9.5)
Nerve ring from anterior end	50 ± 3 (48-54)	60 ± 21 (46-75)	63 ± 5 (59-66)	66 ± 9 (55-73)	62 ± 5 (56-67)
Tail	14.7 ± 3.8 (12.0-19.0)	16 ± 0.1 (16-17)	22 ± 1 (21-22)	27 ± 2.6 (24.5-29.5)	24 ± 2 (23-27)
Anal body diam.	5.2 ± 0.6 (4.0-5.5)	8 ± 1 (7-9)	8 ± 1 (7-8)	11 ± 1 (10-12)	9 ± 1 (8-10)
Genital primordium length (GPL)	11.3 ± 1.6 (9.5-13.5)	137 ± 18 (124-150)	37 ± 10 (30-44)	178 ± 87 (72-284)	138 ± 58 (63-204)
Genital primordium width (GPW)	3.2 ± 0.4 (3.0-4.0)	5.4 ± 1.2 (4.5-6.5)	4.0 ± 1 (4.0-5.0)	8.0 ± 1 (7.0-10.0)	7.0 ± 2 (5.0-9.0)
GPL/GPW	3.6 ± 0.8 (2.4-4.7)	25.6 ± 2.2 (24.0-27.2)	6.0 ± 1 (8.0-9.0)	20.8 ± 7.6 (10.3-28.4)	19.5 ± 4.1 (13.9 ± 23.2)
GPL/L (%)	6 ± 1.0 (5-8)	57 ± 6.0 (53-62)	12 ± 3.0 (10-14)	42 ± 16 (21-61)	37 ± 13 (18-47)
Labial region diam./height	1.5 ± 0.1 (1.4-1.6)	1.9 ± 0.2 (1.7-2.0)	2.0 ± 0.4 (1.7-2.3)	2.0 ± 0.3 (1.7-2.1)	2.0 ± 0.1 (1.9-2.2)
Median bulb length/diam.	1.4 ± 0.1 (1.3-1.5)	1.6 ± 0.5 (1.2-1.9)	1.2 ± 0.1 (1.1-1.2)	1.4 ± 0.1 (1.4-1.5)	1.5 ± 0.1 (1.4-1.6)

Type host, vector and locality

The type host is hybrid walnut trees, *Juglans hindsii* × (*J. nigra* × *J. hindsii*/*J. californica*) (Fagales, Juglandaceae). The type vector is the walnut twig beetle, *Pityophthorus juglandis* (Coleoptera, Curculionidae, Scolytinae), the nematodes initially being found in large clusters attached to the undersides of the elytra of the beetles that were obtained from Sierra Gold Orchard, Sutter County, CA, USA. GPS coordinates (decimal format): 39.051106, −121.613483.

Other localities

Nematodes were also isolated from walnut twig beetles and walnut trees from the following localities: Kerney Agricultural Center, Fresno County, CA, USA, host tree *J. californica*, 09.12.2014, GPS coordinates: 36.6024, −119.5126; Fort Stanton State Monument, Lincoln County, NM, USA, host tree *J. major*, 28.08.2013, GPS coordinates: 33.479891, −105.557256; along HWY 70, Lincoln County, NM, USA, host tree *J. major*, 30.06.2015, GPS coordinates: 33.366417, −105.197133; and near Patagonia, Santa Cruz County, AZ, USA, host tree *J. major*, 06.09.2016, GPS coordinates (decimal format): 31.466111, −110.712222.

Type material

Holotype deposited at the Zoological Institute RAS (Slide N P-4380). Paratypes (every collection slide contains three male and three female paratype nematode specimens) deposited at the University of California, Davis Nematode Collection, Davis, CA, USA. (ten slides); the United States Department of Agriculture Nematode Collection (USDANC), Beltsville, MD, USA (five slides); the Ghent University Museum, Zoology Collection, Ghent, Belgium (five slides); the Forest Pathology Laboratory collection, Forestry and Forest Products Research Institute (FFPRI), Tsukuba, Japan (five slides); the Julius Kühn Institute (JKI), Federal Research Centre for Cultivated Plants, Braunschweig, Germany (five slides); and the Zoological Institute RAS (77 slides, NN P-4381-4457). Living culture on the fungus *B. cinerea* is kept in the Zoological Institute RAS under the culture code: "Subb_Jugl_Calif_2018".

Diagnosis and relationships

Bursaphelenchus juglandis n. sp. belongs to the *Abietinus* group of *Bursaphelenchus* according to the molecular phylogenetic analyses and morphological characters. The new species is characterised by the presence of three lines (*i.e.*, two bands) in the lateral field, small arched vulval flap in female, broad spicule with two lines along blade and small cucullus, digitate dorsally bent condylus and male tail with five papilliform papillae and one pair of glandpapillae P5, and the curved, conical female tail.

From similar species in the *Abietinus* group, *B. juglandis* n. sp. differs in the presence of a cephalic disc with lateral labial sensilla situated at the border of the disc, round ring-like subdorsal amphids and in the thick spicules with the spicule capitulum surface almost parallel to a virtual line extending the spicule end from the dorsal side of spicule blade.

In having three incisures in the lateral field and excretory pore located anteriorly to the nerve ring, *B. juglandis* n. sp. is most similar to *B. irokophilus* Torrini, Strangi, Mazza, Marianelli, Roversi & Kanzaki, 2019 and *B. decraemerae* Wang, Gu, Maria, Fang & Li, 2018a. It differs from *B. irokophilus* in the digitate female tail tip *vs* rounded, c′ = 3.3 (2.6-4.0) *vs* 5.5 (4.9-6.0), blunt rectangular spicule condylus *vs* digitate, and stylet length = 12.0 (11.0-13.0) *vs* 14.8 (13.4-15.7) μm; and from *B. decraemerae* by female c′ = 3.3 (2.6-4.0) *vs* 4.7 (4.3-5.1), c = 18.8 (15.7-22.8) *vs* 12.9 (11.6-14.5), V = 75.0 (72-77) *vs* 68.9 (65.9-71.9), length of PUS (66 (44-110) *vs* 43 (38-47) μm), and the ratio: PUS/vulva-anus distance = 60 (47-80) *vs* 35 (30-39)%.

There are four other *Bursaphelenchus* species phylogenetically close to *B. juglandis* n. sp.: *B. geraerti* Wang, Maria, Gu, Fang, Wang & Li, 2018b, *B. gerberae* Giblin-Davis, Kanzaki, Ye, Center, Thomas, 2006, *B. sakishimanus* Kanzaki, Okabe & Kobori, 2015, and *B. sinensis* Palmisano, Ambrogioni, Tomiczek & Brandstetter, 2004. *Bursaphelenchus juglandis* n. sp. differs from *B. geraerti* in having the excretory pore anterior to the nerve ring *vs* posterior, female c′ = 3.3 (2.6-4.0) *vs* 5.5 (5.0-6.5), condylus rectangular slightly bent dorsally *vs* thumb-like straight continuation of the spicule dorsal outline, cucullus present *vs* absent, two lines on the spicule blade surface *vs* three lines, stylet 12.0 (11.0-13.0) *vs* 13.2 (12.7-14.2) μm, and one pair of gland papillae (P5) *vs* two; from *B. gerberae* in excretory pore positioned anterior to nerve ring *vs* posterior, female c′ = 3.3(2.6-4.0) *vs* 4.8 (4-6), spicule rostrum digitate *vs* pointed, 2 *vs* 3 lines on spicule blade, and female stylet = 12.0 (11.0-13.0) *vs* 14.1 (13-15) μm; from *B. sakishimanus* in female tail hook-like *vs* straight or slightly curved, female c′ = 3.3 (2.6-4.0) *vs* 6.8 (6.1-7.9), condylus rectangular slightly

bent dorsally *vs* digitate bent dorsally, spicule rostrum digitate *v*s pointed, and female stylet = 12.0 (11.0-13.0) *vs* 18.1 (16.4-20.0) μm or longer; and from *B. sinensis* in the broad spicule with wide capitulum and small cucullus *vs* narrow spicule without cucullus with compact capitulum where the condylus and rostrum are fused, three incisures in lateral field *vs* two, hook-like tail in females *vs* straight, spicule length along arc = 11.0 (9.5-12.0) *vs* 19.2 (14.5-21.9) μm, and the PUS/vulva anus distance ratio of 60 (47-80) *vs* 74.9 (62.5-91.5)%.

Bursaphelenchus juglandis n. sp. also resembles *B. hylobianus* (Korenchenko, 1980) Hunt, 1993, but differs by having three incisures in the lateral field *vs* two, spicules 11.0 (9.5-12.0) *vs* 21.5 (20-23) μm long, female stylet length = 12 (11-13) *vs* 15.1 (14-17) μm, two lines along spicule blade *vs* three, and excretory pore located at median bulb or anterior *vs* at nerve ring or posterior.

Sequences of 18S, D2-D3 of 28S and ITS rRNA genes clearly differentiated *B. juglandis* n. sp. from all other species of the *Abietinus* group and from other *Bursaphelenchus* species.

Endoparasites

Three nematode females contained gregarines (Gregarinasina) in the mid-intestine. These individuals were extracted from bark with beetle tunnels (Fig. 5M). However, the gregarine hyperparasites were not detected in the intestines of nematodes extracted from agar cultures grown on *B. cinerea*.

Host-parasite relations and pathogenicity

The insect vector is the walnut twig beetle, *P. juglandis*, one of the agents of TCD with the fungus *G. morbida*, which is vectored by the beetle. The fungus causes cankers around the beetle galleries in the phloem. Nematodes are also vectored by the beetles and thus they may be involved as the agents in the canker disease process.

Molecular characterisation and phylogenetic position

The D2-D3 of 28S rRNA gene alignment (923 bp) included 94 sequences of *Bursaphelenchus* and two sequences of *Panagrolaimus* and *Panagrellus*, which were selected as outgroup taxa. Phylogenetic analysis resulted in the Bayesian consensus tree in Figure 10. *Bursaphelenchus juglandis* n. sp. was supported (100%) as part of a clade with *B. decraemerae* and *B. geraerti*. Its sequence differs from those species by 9.3% (65 bp) and 11.6% (82 bp), respectively.

The partial 18S rRNA gene alignment (1724 bp) included 86 sequences of *Bursaphelenchus* and two sequences of *Aphelenchoides stammeri* (Körner, 1954) Hunt, 1993 and *Robustodorus megadorus* (Allen, 1941) Andrássy, 2007 (selected as outgroup taxa). The 18S Bayesian consensus tree is given in Figure 11. The new species showed unresolved relationship with several groups of *Bursaphelenchus*. The sequence of the new species differs from that of *B. geraerti* by 1.8% (14 bp).

The automatic ITS rRNA gene sequence alignment included 30 sequences of *Bursaphelenchus* and was 1768 bp in length, whereas the culled alignment was 551 bp in length. The Bayesian consensus trees are presented in Figure 12A; B. *Bursaphelenchus juglandis* n. sp. forms strongly or moderately supported clades with *B. sinensis*.

Molecular diagnostics

A species-specific primer was developed for *B. juglandis* n. sp. based on differences in the ITS rRNA gene sequences. Results of PCR with the species-specific primers are given in Figure 13. The combination of the universal forward primer F194 with the species-specific reverse primer ITS-jugR2 yielded a PCR product of *ca* 190 bp for *B. juglandis* n. sp. No amplification occurred with samples of other *Bursaphelenchus* species and a negative control without DNA.

The *Abietinus* group (emended diagnosis)

Lateral fields with one band (two incisures) or two bands divided by shallow groove (three incisures but the central one is weak). Valve in median bulb well developed, central. Excretory pore usually anterior to nerve ring, occasionally at level of nerve ring. Head high hemispherical, set off by constriction from neck.

Male

Spicules paired, symmetrical, with small disc-like cucullus at tip, which is sometimes indistinct. Spicules broad almost rhomboid, condylus 25% of spicule length, conical with digitate or narrowly conical apex, rostrum triangular with digitate ending. Spicule blade with one flange (two incisures, sometimes three incisures) extending along its lateral surface. Tail with seven caudal papillae of two types: papilliform (5) and glandpapillae (2 or 4). Papilliform papillae comprising unpaired P1 just anterior to

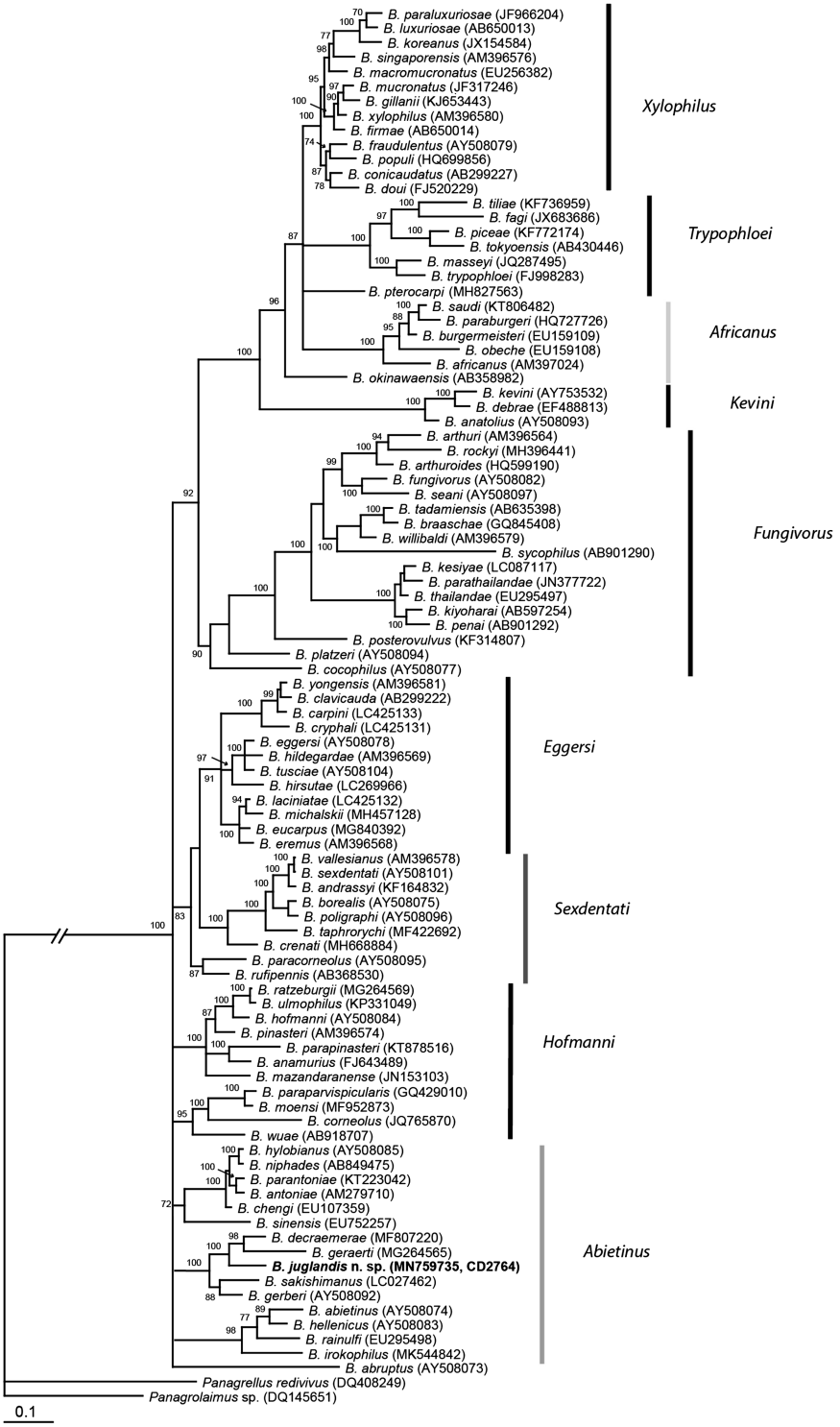

Fig. 10. Phylogenetic relationships within *Bursaphelenchus* spp. as inferred from Bayesian analysis of the D2-D3 expansion segments of 28S rRNA gene sequences. Posterior probability values more than 70% are given on appropriate clades. New sequence indicated in bold. *Bursaphelenchus* grouping is given according to Ryss & Subbotin (2017) with modifications.

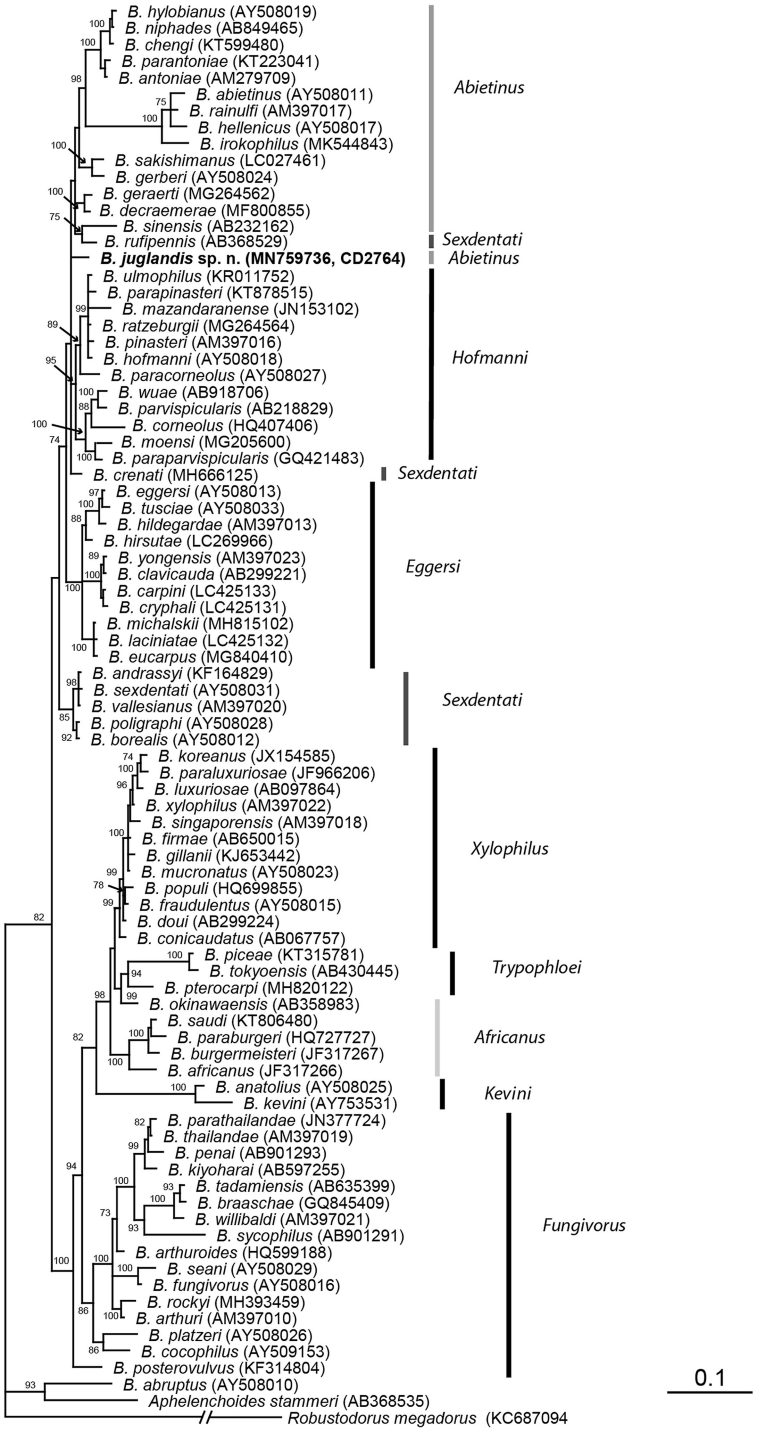

Fig. 11. Phylogenetic relationships within *Bursaphelenchus* spp. as inferred from Bayesian analysis of the partial 18S rRNA gene sequences. Posterior probability values more than 70% are given on appropriate clades. New sequence indicated in bold. *Bursaphelenchus* grouping is given according to Ryss & Subbotin (2017) with modifications.

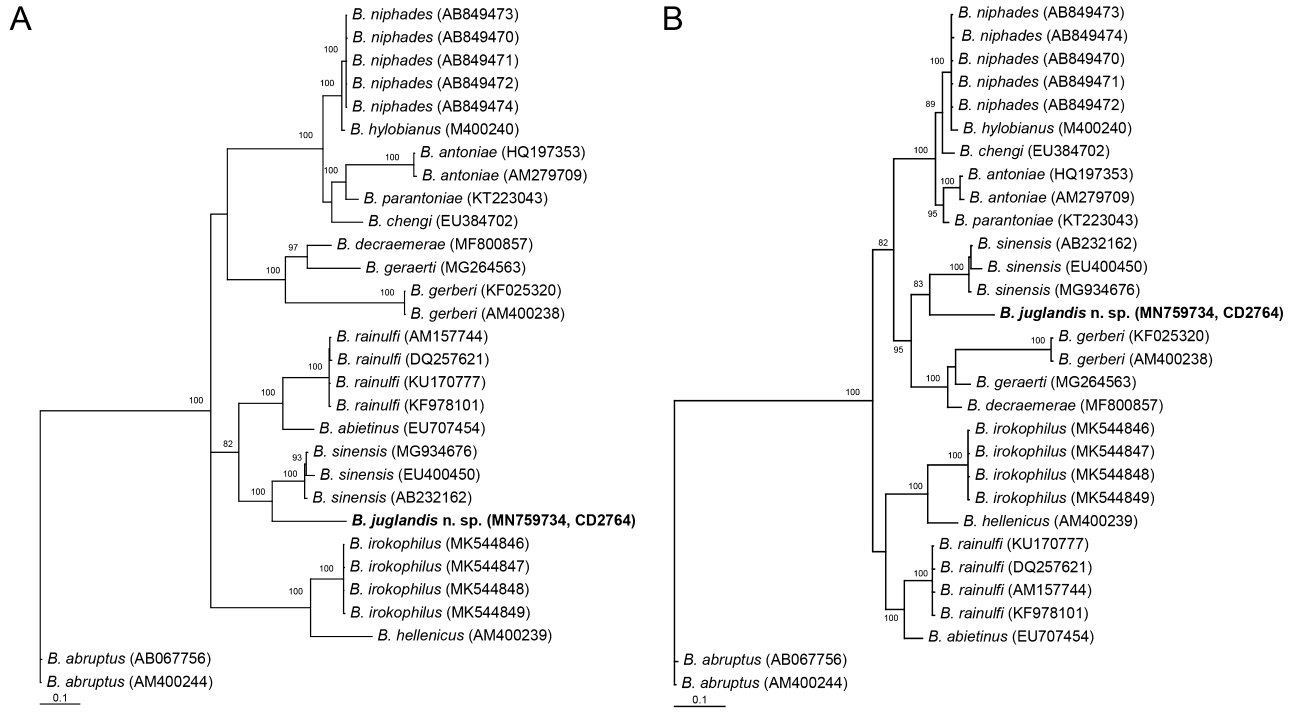

Fig. 12. Phylogenetic relationships within *Bursaphelenchus* of the *Abietinus* group as inferred from Bayesian analysis of the partial ITS rRNA gene sequences. A: Phylogenetic tree reconstructed from a full length automatic alignment (1768 bp); B: Phylogenetic tree reconstructed from a culled alignment (551 bp) obtained after eliminating poorly aligned segments. Posterior probability values more than 70% are given on appropriate clades. New sequence are indicated in bold.

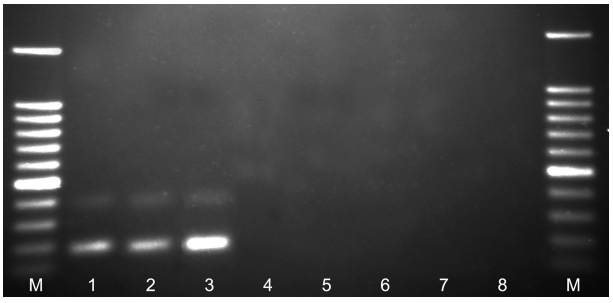

Fig. 13. Gel with specific amplicons obtained from PCR with the universal forward primer and species-specific primer. Lanes: M = 100 bp DNA ladder (Promega); 1, 2 = *Bursaphelenchus juglandis* n. sp. (CD2971) obtained from fungus culture; 3 = *B. juglandis* n. sp. (California, USA, CD2764) obtained from wood sample; 4 = *B. mucronatus* (Russia, CD1409); 5 = *B. crenati* (Belorussia, CD2761); 6 = *B. ulmophilus* (Russia, CD1705); 7 = *B. fraudulentus* (Russia, CD2935); 8 = control without DNA.

cloacal opening, paired P2 situated ventrolateral at same level or slightly posterior to cloacal opening, and paired P3 at mid-tail or slightly posterior. An additional pair of gland papillae (GP5) are the minute round or slit-like pores on small oval plates or fused heart-like plate situated at ventral tail midline near junction of tail tip and the 6-10 μm long bursal flap. Sometimes additional paired GP6 glandpapillae may be seen on the oval plates just posterior to GP5. One pair (P4 papilliform), which is present in the *Kevini* and *Fungivorus* groups, is absent in the *Abietinus* group. Caudal papilla formula: P1 + P2, P3, GP (5,6).

Female

Vulva a small arched vulval flap with 2-3 μm lateral wings and rounded swollen posterior vulval lip usually bearing narrow transverse band. Short cuticular vagina sloping ventrally. PUS usually forming 50% or more of vulva-anus distance. Tail narrow, usually hook-like with ventrally curved narrow digitate or bearing thick set off mucron. Life cycle trixenic with transmission (insect vectored) and propagative generations. Propagative generations of nematodes feeding on fungal mycelium, nematodes present in inner bark, rotten cambium and sapwood

of dying tree hosts, and within beetle tunnels under bark. The transmission generation dauer stage is vectored under elytra of beetles of the family Curculionidae, subfamilies Curculioninae and Scolytinae. Plant hosts are coniferous and deciduous trees.

Species list of the *Abietinus* group

Bursaphelenchus abietinus Braasch & Schmutzenhofer, 2000
B. antoniae Penas, Metge, Mota & Valadas, 2006
B. chengi Li, Trinh, Waeyenberge & Moens, 2008
B. decraemerae Wang, Gu, Maria, Fang & Li, 2018a
B. geraerti Wang, Maria, Gu, Fang, Wang & Li, 2018b
B. gerberae Giblin-Davis, Kanzaki, Ye, Center & Thomas, 2006
B. hellenicus Skarmoutsos, Braasch & Michalopoulou, 1998
B. hylobianus (Korenchenko, 1980) Hunt, 1993
= *Parasitaphelenchus hylobianus* Korenchenko, 1980
B. irokophilus Torrini, Strangi, Mazza, Marianelli, Roversi & Kanzaki, 2019
B. juglandis n. sp.
B. niphades Tanaka, Tanaka, Akiba, Aikawa, Maehara, Takeuchi & Kanzaki, 2014
B. parantoniae Maria, Fang, He, Gu & Li, 2015
B. pityogeni Massey, 1974
B. rainulfi Braasch & Burgermeister, 2002
B. sakishimanus Kanzaki, Okabe & Kobori, 2015
B. sinensis Palmisano, Ambrogioni, Tomiczek & Brandstetter, 2004
B. varicauda Thong & Webster, 1983
B. willi (Massey, 1974) Baujard, 1989
= *Teragramia willi* Massey, 1974

Comments

Bursaphelenchus pityogeni, *B. varicauda* and *B. willi* lack molecular data and are absent in the phylogenetic cladograms; however, they were referred to the *Abietinus* group by Braasch *et al*. (2009).

A tabular polytomous diagnostic key to species of the *Abietinus* group is given in Table 4. Lists of vectors, plant hosts and distribution for species of the *Abietinus* group is presented in Supplementary Table S1.

Discussion

Relationships of the *Abietinus* group within other *Bursaphelenchus*

According to the Ryss & Subbotin (2017) classification, the *Abietinus* group belongs to macroclade C of *Bursaphelenchus*, which differs from the other macroclades (A and B) in the pattern of the male caudal papillae and presence of a small arched vulval flap. Papilla formula: papilliform papillae: unpaired P1 + paired P2 at level of caudal opening, paired P3 at mid-tail, glandpapillae: paired GP5 or GP5 + GP6, each glandpapilla either situated on a minute oval plate close to the ventral midline at the base of prominent bursal flap, or both glandpapillae situated on a fused heart-like plate.

There are five species groups belonging to macroclade C: *Abietinus*, *Eggersi*, *Hylobianus*, *Hofmanni*, and *Sexdentati* (Ryss & Subbotin, 2017). The *Abietinus* group differs from the *Sexdentati* group by two or three lateral lines *vs* four lines in *Sexdentati*. The *Eggersi* group differs from the *Abietinus* group in spicule shape: small capitulum with small reversed condylus *vs* broad capitulum with long conical condylus, and cucullus absent in *Eggersi vs* small disc-like cucullus present in the *Abietinus* and *Hofmanni* groups. Males of the *Hofmanni* group have four lines along the spicule blade *vs* mostly two lines (one flange) in spicules of the *Abietinus* group. Spicules of the *Abietinus* group have a long conical condylus *ca* 25% of spicule length *vs* small rounded condylus in the *Hofmanni* group.

Tanaka *et al*. (2014) proposed the '*Hylobianum*' group (= *Hylobianus* group as the correct name of '*B. hylobianum*', according to Hunt (2008), is *B. hylobianus*) for four phylogenetically clustered species: *B. hylobianus*, *B. antoniae*, *B. niphades* and *B. chengi*. Maria *et al*. (2015) added *B. parantoniae* to the *Hylobianus* group. The first three mentioned species in the group are vectored by Curculioninae weevils, but the natural insect associates are currently unknown for *B. parantoniae* and *B. chengi*. Ryss & Subbotin (2017) considered the *Hylobianus* group as a phylogenetically and morphologically based group of two species: *B. hylobianus* and *B. paracorneolus* Braasch, 2000, both being associated with coniferous plant hosts. However, the phylogenetic trees given in the present paper (Figs 10-12) did not reveal a distinct lineage for the *Hylobianus* group, which may be considered as distinctly different from the *Abietinus* group. Other *Hylobianus* group features, including the male spicule being angular and broad with an extremely long dorsally curved massive

Table 4. Tabular identification key to *Bursaphelenchus* species of the *Abietinus* group.

Species	Character												
	C1	C2	C3	C4	C5	C6	C7	C8	C9	C10	C11	C12	C13
B. abietinus	3	1	1	3	12	1	3	1	3	2	1	23	?
B. antoniae	3	1	2	2	3	3	3	1	2	2	2	23	1
B. chengi	3	1	1	2	3	1	3	2	2	2	2	2	2
B. decraemerae	2	2	1	2	3	3	3	1	3	2	1	3	1
B. geraerti	2	1	1	2	3	4	4	2	3	3	1	2	2
B. gerberae	2	1	1	2	3	3	2	1	3	3	1	2	1
B. hellenicus	3	1	3	3	2	1	4	1	23	2	1	2	1
B. hylobianus	3	12	1	2	23	12	4	1	2	3	2	2	2
B. irokophilus	2	2	1	3	3	1	3	1	3	2	1	2	1
B. juglandis n. sp.	2	2	1	2	2	3	3	1	3	2	1	3	1
B. niphades	3	1	2	3	3	3	3	1	2	3	1	2	2
B. parantoniae	3	1	2	2	3	3	3	1	23	3	2	2	1
B. pityogeni	3	2	2	3	1	2	2	2	23	1	2	2	?
B. rainulfi	3	3	1	2	3	1	3	2	3	2	1	2	1
B. sakishimanus	2	3	2	2	3	1	2	1	3	2	1	1	1
B. sinensis	3	2	2	12	2	4	4	2	2	1	2	23	1
B. varicauda	?	1	3	13	1	1	4	2	23	2	2	2	1
B. willi	3	2	3	4	3	1	2	2	12	1	1	3	?

Character definitions:

C1: Number of lateral field incisures. 1: 4; 2: 3; 3: 2
C2: Excretory pore position: 1: posterior to nerve ring; 2: at nerve ring or between nerve ring and median bulb; 3: at median bulb.
C3: Tail shape in female. 1: conical, hook-like; 2: conical, straight or very slightly curved; 3: subconical; 4: subcylindrical; 5: cylindrical.
C4: Tail tip shape in female. 1: mucronate; 2: conical to digitate; 3: rounded; 4: hemispherical.
C5: c′-value in female. 1: 2-3; 2: 3-4; 3: >4.
C6: Spicule condylus. 1: digitate bent dorsally; 2: rectangular with backward process; 3: rectangular, slightly bent dorsally; 4: thumb-like, straight continuation of the spicule dorsal outline.
C7: Spicule rostrum. 1: thorn-like; 2: pointed; 3: digitate; 4: triangular blunt.
C8: Spicule tip. 1: cucullus present; 2: cucullus absent.
C9: Spicule length along arc. 1: $\geqslant$26 μm; 2: 16-25 μm; 3: $\leqslant$15 μm.
C10: Number of ridges (lines) on spicule blade 1: 1; 2: 2; 3: 3; 4: 4.
C11: Post-vulval uterine sac length as % of vulva-anus distance. 1: $\leqslant$60%; 2: >60%.
C12: Stylet length in female. 1: 18 μm or longer; 2: 13-17 μm; 3: $\leqslant$12 μm.
C13: Gland papillae at tail tip of male just anterior to bursal flap. 1: one pair (P5); 2: two pairs (P5 + P6) or 3 pairs.

condylus, three lines on the spicule blade, small disc-like cucullus, two or three incisures in the lateral field, excretory pore at nerve ring or anterior, general body and female tail shape, and the host and vector ranges do not distinguish species of the *Hylobianus* group from those of the *Abietinus* group. Thus, we consider all species of the *Hylobianus* group as representatives of the *Abietinus* group.

It was difficult to attribute the relationship of *B. sinensis*, which was placed by various authors in different groups and positions to other *Bursaphelenchus* group lineages. Braasch *et al*. (2009) considered *B. sinensis* as a separate monospecies group within the two-incisure section of *Bursaphelenchus*. The decision was based on the narrow spicule shape with a compact capitulum where the condylus and rostrum are fused and the ventral limb of the blade membrane-like and devoid of flanges. Kanzaki *et al*. (2019) and Kanzaki & Giblin-Davis (2020) discovered morphological and biological dimorphism of *B. sinensis* expressed as two forms: a common fungal-feeding form and the *Ektaphelenchus*-like predatory form in females appearing in the population when fungal food sources

are limited but potential prey nematode species are available. These authors attributed this species to the *Aberrans* group, which was proposed by Ryss *et al*. (2005) basing on its morphological similarities and presence of narrow spicules with a compact capitulum. Moreover, Kanzaki *et al*. (2019) considered the facultative predatory form in the declining population as a biological character of the *Aberrans* group. However, the results of phylogenetic analyses obtained here and published by other authors (Wang *et al*., 2018a, b; Gu *et al.*, 2019) showed that *B. sinensis* belongs to the *Abietinus* group. The morphology of the species fits well with the *Abietinus* group diagnosis with the only exception being the spicule shape. Taking account of the adaptive flexibility in morphology (*e.g.*, feeding predatory dimorphism of mycophagous and predatory forms within one population, reduction of feeding structures in dauers), spicule shape is an important character but not the main structure to classify the *Bursaphelenchus* spp. It would be desirable to use a set of characters, some of which may deviate from the diagnosis of the group.

Bursaphelenchus juglandis n. sp. in phylogenetic trees

Molecular phylogenetic analyses using the D2-D3 expansion segments of 28S rRNA and ITS rRNA gene sequences placed *B. juglandis* n. sp. into the *Abietinus* group. *Bursaphelenchus juglandis* n. sp. showed a sister relationship with *B. decraemerae* and *B. geraerti* in the 28S rRNA gene phylogenetic tree, whereas it formed a clade with *B. sinensis* in the ITS rRNA gene phylogenetic trees. In the ITS rRNA gene tree reconstructed from the culled alignment, *B. juglandis* n. sp. and *B. sinensis* were in a subclade with *B. decraemerae*, *B. geraerti* and *B. gerberi*. The position of *B. juglandis* n. sp. within *Bursaphelenchus*, as inferred from the analysis of partially sequenced 18S rRNA gene, was also still uncertain, probably because of a low phylogenetic signal in this marker.

Juvenile characters in systematics

Morphological characters of the juveniles may help in species diagnostics and understanding of the phylogenetic relations of *Bursaphelenchus* spp. The diagnostics of the developmental stages and sex in the propagative juveniles of *B. juglandis* n. sp. may be based on the following most important characters: the body morphometric indices, genital primordium size and shape, as well as the tail shape. This characterisation was key in attributing the dauer juveniles of *B. juglandis* n. sp., located in clusters under elytra of the bark beetle, as the DJ3 and to find differences between male and female dauers in tail tip shape and the presence of a cloacal primordium in male juveniles. The female DJ3 of *B. juglandis* n. sp. has a distinct mucronate tail, which may differentiate this species from close relatives. The DJ3 in species of *Abietinus* group is an additional difference from the *Xylophilus* group, in which species are characterised by a DJ4 dauer. Both groups also differ in their vectors: the *Abietinus* group species use Curculionidae vectors whereas those of the *Xylophilus* group are vectored by Cerambycidae. The target stage of vector for the *Xylophilus* group is the pupa or imago of longhorn beetles, which appear in spring; thus the period to contact the vector is very short for the dauer, whereas dauers of *Abietinus* group species may be found in imagos, pupae and mature larvae of the vector in winter. Because of this, the dauer stage in the *Xylophilus* group is the later stage juvenile (DJ4) as opposed to the DJ3 stage in the groups vectored by bark beetles.

Possible role of the nematodes in the pathogenic association

The insect vector of *B. juglandis* n. sp. is the walnut twig beetle, *P. juglandis*. The beetle is one of the agents of TCD along with the fungus *G. morbida*. This beetle is native to the southern part of the USA (New Mexico, Arizona), and Mexico. However, the beetle is now an invasive species over all of the western USA, and is in the process of invading the eastern half of the country (Rugman-Jones *et al*., 2015). These beetles are primarily attracted to species of black walnut and butternut, rather than the Persian or English walnut used in commercial walnut production, but they are opportunistic. They use an aggregation pheromone to colonise host trees in large numbers, often focusing on specific branches. The *G. morbida* fungus creates cankers around the numerous beetle galleries in the phloem, which coalesce and effectively girdle and then kill the branch. Repeated colonisations over multiple years can ultimately kill the host tree.

Among the species of the *Abietinus* group, *B. juglandis* n. sp. is the only one that may be a part of a pathogenic association causing a disease of commercial woody plants; the same beetle vector is common both for the pathogenic fungus and nematode transmission stages. To understand the role of the new species in TCD it is necessary to carry out additional studies and pathogenicity tests. Of special interest may be the study of the relations between *B. juglandis* n. sp. with *G. morbida* dur-

ing transmission and within the infected tree host, as already reported for some *Bursaphelenchus* species and plant pathogenic fungi, *e.g.*, *B. trypophloei* Tomalak & Filipiak, 2011 and *Cytospora chrysorrhoea* Pers. (Tomalak & Filipiak, 2011), *B. masseyi* Tomalak, Worrall & Filipiak, 2013 and *C. chrysorrhoea* (Tomalak *et al*., 2013), and *B. fraudulentus* Rühm, 1956 and *Armillaria ostoyae* (Romagn.) Herink (Tomalak, 2017).

Acknowledgements

The study was supported for the first and last authors by a grant from the Russian Foundation for Basic Research 20-04-00569 A 'Evolution, phylogeny and the ways of life cycle alteration of the wood and bark inhabiting nematodes (Nematoda: Rhabditida: Tylenchina and Rhabditina) during natural and anthropogenic transformation of ecosystems'. Sergio Álvarez-Ortega thanks "AYUDA PUENTE 2019, URJC" of the Universidad Rey Juan Carlos for financial support.

References

Akbulut, S., Braasch, H. & Cebeci, H.H. (2013). First report of *Bursaphelenchus hellenicus* Skarmoutsos, Braasch, Michalopoulou 1998 (Nematoda: Aphelenchoididae) from Turkey. *Forest Pathology* 43, 402-406. DOI: 10.1111/efp.12045

Álvarez-Ortega, S. & Peña-Santiago, R. (2016). *Aporcella charidemiensis* sp. n. (Dorylaimida: Aporcelaimidae) from the southern Iberian Peninsula, with comments on the phylogeny of the genus. *Nematology* 18, 811-821. DOI: 10.1163/15685411-00002995

Ambrogioni, L., Irdani, T. & Caroppo, S. (2003). Records of *Bursaphelenchus* species on coniferous wood imported from Asian Russia and China to Italy. *Redia* 86, 139-146.

Arias, M., Escuer, M. & Bello, A. (2004). [Nematodes associated with conifer wood in Spanish pine forests.] *Boletin de Sanidad Vegetal, Plagas* 30, 581-593.

Baujard, P. (1989). Remarques sur les genres des sous-familles Bursaphelenchinae Paramonov, 1964 et Rhadinaphelenchinae Paramonov, 1964 (Nematoda: Aphelenchoididae). *Revue de Nématologie* 12, 323-324.

Braasch, H. & Braasch-Bidasak, R. (2002). First record of the genus *Bursaphelenchus* Fuchs, 1937 in Thailand and description of *B. thailandae* sp. n. (Nematoda: Parasitaphelenchidae). *Nematology* 4, 853-863. DOI: 10.1163/156854102760402621

Braasch, H. & Burgermeister, W. (2002). *Bursaphelenchus rainulfi* sp. n. (Nematoda: Parasitaphelenchidae), first record of the genus *Bursaphelenchus* Fuchs, 1937 from Malaysia. *Nematology* 4, 971-978. DOI: 10.1163/156854102321122593

Braasch, H. & Schmutzenhofer, H. (2000). *Bursaphelenchus abietinus* sp. n. (Nematoda: Parasitaphelenchidae) associated with fir bark beetles (*Pityokteines* spp.) from declining trees in Austria. *Russian Journal of Nematology* 8, 1-6.

Braasch, H., Metge, K. & Burgermeister, W. (1999). *Bursaphelenchus*-Arten (Nematoda, Parasitaphelenchidae) in Nadelgehölzen in Deutschland und ihre ITS-RFLP-Muster. *Nachrichtenblatt des Deutschen Pflanzenschutzdienstes* 51, 312-320.

Braasch, H., Tomiczek, C., Metge, K., Hoyer, U., Burgermeister, W., Wulfert, I. & Shönefeld, U. (2001). Records of *Bursaphelenchus* spp. (Nematoda, Parasitaphelenchidae) in coniferous timber imported from the Asian part of Russia. *Forest Pathology* 31, 129-140. DOI: 10.1046/j.1439-0329.2001.00233.x

Braasch, H., Burgermeister, W. & Gu, J. (2009). Revised intrageneric grouping of *Bursaphelenchus* Fuchs, 1937 (Nematoda: Aphelenchoididae). *Journal of Nematode Morphology and Systematics* 12, 65-81.

Calin, M., Costache, C., Braasch, H., Zaulet, M., Buburuzan, L., Petrovan, V., Dumitru, M., Mota, M. & Vieira, P. (2015). New reports of *Bursaphelenchus* species associated with conifer trees in Romania. *Forest Pathology* 45, 239-245. DOI: 10.1111/efp.12163

Carletti, B. (2008). *Bursaphelenchus* species with natural vectors in Italy: distribution and essential diagnostic features. *Redia* 91, 111-117.

Carta, L.K. & Wick, R.L. (2018). First report of *Bursaphelenchus antoniae* from *Pinus strobus* in the U.S. *Journal of Nematology* 50, 473-478. DOI: 10.21307/jofnem-2018-052

Chizhov, V.N., Chumakova, O.A., Subbotin, S.A. & Baldwin, J.G. (2006). Morphological and molecular characterization of foliar nematodes of the genus *Aphelenchoides*: *A. fragariae* and *A. ritzemabosi* (Nematoda: Aphelenchoididae) from the Main Botanical Garden of the Russian Academy of Sciences, Moscow. *Russian Journal of Nematology* 14, 179-184.

Dan, Y. & Yu, S.F. (2003). Identification of *Bursaphelenchus* spp. on pine wood in Yunnan Province. *Acta Phytopathologica Sinica* 33, 401-405.

Dereeper, A., Guignon, V., Blanc, G., Audic, S., Buffet, S., Chevenet, F., Dufayard, J.F., Guindon, S., Lefort, V., Lescot, M. *et al.* (2008). Phylogeny.fr: robust phylogenetic analysis for the non-specialist. *Nucleic Acids Research* 36 (Web Server issue), W465-W469. DOI: 10.1093/nar/gkn180

d'Errico, G., Carletti, B., Schroder, T., Mota, M., Vieira, P. & Roversi, P.F. (2015). An update on the occurrence of nematodes belonging to the genus *Bursaphelenchus* in the Mediterranean area. *International Journal of Forest Research* 88, 1-12. DOI: 10.1093/forestry/cpv028

Escuer, M., Árias, M. & Bello, A. (2004). Occurrence of the genus *Bursaphelenchus* Fuchs, 1937 (Nematoda: Aphelenchida) in Spanish conifer forests. *Nematology* 6, 155-156. DOI: 10.1163/156854104323073035

Ferris, V.R., Ferris, J.M. & Faghihi, J. (1993). Variation in spacer ribosomal DNA in some cyst-forming species of plant parasitic nematodes. *Fundamental and Applied Nematology* 16, 177-184.

Giblin-Davis, R.M., Kanzaki, N., Ye, W., Center, B.J. & Thomas, K. (2006). Morphology and systematics of *Bursaphelenchus gerberae* n. sp. (Nematoda: Parasitaphelenchidae), a rare associate of the palm weevil, *Rhynchophorus palmarum* in Trinidad. *Zootaxa* 1189, 39-53. DOI: 10.11646/zootaxa.1189.1.2

Gu, J., Chen, X.-F., Zheng, W., Wen, W.-G. & Zheng, J.-W. (2009). [Characterization of *Bursaphelenchus chengi* Li, Trinh, Waeyenberge & Moens, 2008 from wood packaging of *Pinus taiwanensis* in Ningbo, China.] *Journal of Zhejiang University (Agricultural & Life Sciences)* 35, 383-389.

Gu, J.F., Braasch, H., Burgermeister, W. & Zhang, J.C. (2006). Records of *Bursaphelenchus* spp. intercepted in imported packaging wood at Ningbo, China. *Forest Pathology* 36, 323-333. DOI: 10.1111/j.1439-0329.2006.00462.x

Gu, J.F., Fang, Y., Liu, L., Pedram, M. & Li, H. (2019). *Bursaphelenchus pterocarpi* n. sp. (Tylenchina: Aphelenchoididae) found in *Pterocarpus* sp. imported into China from Ghana. *Nematology* 21, 725-737. DOI: 10.1163/15685411-00003248

Hunt, D.J. (1993). *Aphelenchida, Longidoridae and Trichodoridae: their systematics and bionomics*. Wallingford, UK, CAB International.

Hunt, D.J. (2008). A checklist of the Aphelenchoidea (Nematoda: Tylenchina). *Journal of Nematode Morphology and Systematics* 10(2007), 99-135.

Jiang, L.Q., Li, X.Q. & Zheng, J.W. (2007). First record of *Bursaphelenchus rainulfi* on pine trees from eastern China and its phylogenetic relationship with intro-genus species. *Journal of Zhejiang University Science B* 8, 345-351.

Kanzaki, N. & Futai, K. (2007). Isolation of *Bursaphelenchus sinensis* (Nematoda: Parasitaphelenchidae) from dead Japanese black pine, *Pinus thunbergii* Parl. in Japan. *Journal of Nematode Morphology and Systematics* 9, 129-136.

Kanzaki, N. & Giblin-Davis, R.M. (2018). Diversity and plant pathogenicity of *Bursaphelenchus* and related nematodes in relation to their vector bionomics. *Current Forestry Reports* 4, 85-100. DOI: 10.1007/s40725-018-0074-7

Kanzaki, N. & Giblin-Davis, R.M. (2020). The genus *Berntsenus* Massey, 1974 is a junior synonym of *Bursaphelenchus* Fuchs, 1937. *Nematology* 22, 677-695. DOI: 10.1163/15685411-00003332

Kanzaki, N., Okabe, K. & Kobori, Y. (2015). *Bursaphelenchus sakishimanus* n. sp. (Tylenchomorpha: Aphelenchoididae) isolated from a stag beetle, *Dorcus titanus sakishimanus* Nomura (Coleoptera: Lucanidae), on Ishigaki Island, Japan. *Nematology* 17, 531-542. DOI: 10.1163/15685411-00002887

Kanzaki, N., Ekino, T., Ide, T., Masuya, H. & Degawa, Y. (2018). Three new species of parasitaphelenchids, *Parasitaphelenchus frontalis* n. sp., *P. costati* n. sp. and *Bursaphelenchus hirsutae* n. sp. (Nematoda: Aphelenchoididae), isolated from bark beetles from Japan. *Nematology* 20, 957-1005. DOI: 10.1163/15685411-00003189

Kanzaki, N., Ekino, T. & Giblin-Davis, R.M. (2019). Feeding dimorphism in a mycophagous nematode, *Bursaphelenchus sinensis*. *Scientific Reports* 9, 13956. DOI: 13910.11038/s41598-13019-50462-z

Kolarik, M., Freeland, E., Utley, C. & Tisserat, N. (2011). *Geosmithia morbida* sp. nov., a new phytopathogenic species living in symbiosis with the walnut twig beetle (*Pityophthorus juglandis*) on *Juglans* in USA. *Mycologia* 103, 325-332. DOI: 10.3852/10-124

Korenchenko, E.A. (1980). [New species of nematodes from the family Aphelenchoididae, parasites of stem pests of the Dahurian larch.] *Zoologicheskii Zhurnal* 59, 1768-1780.

Li, H., Trinh, P.Q., Waeyenberge, L. & Moens, M. (2008). *Bursaphelenchus chengi* sp. n. (Nematoda: Parasitaphelenchidae) isolated at Nanjing, China, in packaging wood from Taiwan. *Nematology* 10, 335-346. DOI: 10.1163/156854108783900294

Li, H., Trinh, P.Q., Waeyenberge, L. & Moens, M. (2009). Characterisation of *Bursaphelenchus* spp. isolated from packaging wood imported at Nanjing, China. *Nematology* 11, 375-408. DOI: 10.1163/156854109X446971

Maria, M., Fang, Y., He, J., Gu, J. & Li, H. (2015). *Bursaphelenchus parantoniae* n. sp. (Tylenchina: Aphelenchoididae) found in packaging wood from Belgium. *Nematology* 17, 1141-1152. DOI: 10.1163/15685411-00002929

Massey, C.L. (1974). *Biology and taxonomy of nematode parasites and associates of bark beetles in the United States*. *Agriculture Handbook No. 446*. Washington, DC, USA, USDA Forest Service.

Nguyen, T.T., Tan, J.J., Ye, J.R. & Lin, S.X. (2016). A survey on the symptoms and endoparasite of the dead pine trees in Vietnam. *Journal of Nanjing Forestry University (Natural Sciences Edition)* 40, 44-52.

Palmisano, A.M., Ambrogioni, L., Tomiczek, C.H. & Brandstetter, M. (2004). *Bursaphelenchus sinensis* sp. n. and *B. thailandae* Braasch *et* Braasch-Bidasak in packaging wood from China. *Nematologia Mediterranea* 32, 57-65.

Pedram, M., Pourjam, E., Ye, W., Robbins, R.T., Atighi, M.R. & Ryss, A. (2011). Description of *Bursaphelenchus mazandaranense* sp. n. (Nematoda: Parasitaphelenchidae) from Iran. *Russian Journal of Nematology* 19, 121-129.

Peña-Santiago, R., Abolafia, J. & Álvarez-Ortega, S. (2014). New proposal for a detailed description of the dorylaim spicule (Nematoda: Dorylaimida). *Nematology* 16, 1091-1095. DOI: 10.1163/15685411-00002834

Penas, A.C., Correia, P., Bravo, M.A., Mota, M. & Tenreiro, R. (2004). Species of *Bursaphelenchus* Fuchs, 1937 (Nematoda: Parasitaphelenchidae) associated with maritime pine in Portugal. *Nematology* 6, 437-453. DOI: 10.1163/1568541042360573

Penas, A.C., Metge, K., Mota, M. & Valadas, V. (2006). *Bursaphelenchus antoniae* sp. n. (Nematoda: Parasita-

phelenchidae) associated with *Hylobius* sp. from *Pinus pinaster* in Portugal. *Nematology* 8, 659-669. DOI: 10.1163/156854106778877947

Penas, A.C., Bravo, M.A., Valadas, V. & Mota, M. (2008). Detailed morphobiometric studies of *Bursaphelenchus xylophilus* and characterisation of other *Bursaphelenchus* species (Nematoda: Parasitaphelenchidae) associated with *Pinus pinaster* in Portugal. *Journal of Nematode Morphology and Systematics* 10, 137-163.

Qin, F.N. & Pan, C.S. (2005). Studies on pine-parasitic nematodes in Fujian. I. Species of *Bursaphelenchus* genus on pine stem. *Journal of Xiamen University (Natural Science)* 44, 723-728.

Ronquist, F. & Huelsenbeck, J.P. (2003). MRBAYES 3 Bayesian phylogenetic inference under mixed models. *Bioinformatics* 19, 1572-1574. DOI: 10.1093/bioinformatics/btg180

Rugman-Jones, P.F., Seybold, S.J., Graves, A.D. & Stouthamer, R. (2015). Phylogeography of the walnut twig beetle, *Pityophthorus juglandis*, the vector of thousand cankers disease in North American walnut trees. *PLoS ONE* 10, e0118264. DOI: 10.1371/journal.pone.0118264

Ryss, A., Vieira, P., Mota, M. & Kulinich, O. (2005). A synopsis of the genus *Bursaphelenchus* Fuchs, 1937 (Aphelenchida: Parasitaphelenchidae) with keys to species. *Nematology* 7, 393-458. DOI: 10.1163/156854105774355581

Ryss, A., Polyanina, K.S., Popovichev, B.G. & Subbotin, S.A. (2015). Description of *Bursaphelenchus ulmophilus* sp. n. (Nematoda: Parasitaphelenchinae) associated with Dutch elm disease of *Ulmus glabra* Huds. in the Russian North West. *Nematology* 15, 685-703. DOI: 10.1163/15685411-00002902

Ryss, A.Y. (2015). [The most simple techniques for detection and laboratory cultivation of woody plant wilt nematodes.] *Izvestia Sankt-Peterburgskoj Lesotehnicheskoj Akademii* 211, 287-295.

Ryss, A.Y. (2017a). A simple express technique to process nematodes for collection slide mounts. *Journal of Nematology* 49, 27-32. DOI: 10.21307/jofnem-2017-043

Ryss, A.Y. (2017b). The simplest « field » methods for extraction of nematodes from plants, wood, insects and soil, with additional description how to keep extracted nematodes alive for a long time. *Parazitologiya* 51, 57-67.

Ryss, A.Y. & Subbotin, S.A. (2017). [Coevolution of wood-inhabiting nematodes of the genus *Bursaphelenchus* Fuchs, 1937 with their insect vectors and plant hosts.] *Zhurnal Obshchei Biologii* 78, 13-42.

Ryss, A.Y., McClure, M.A., Nischwitz, C., Dhiman, C. & Subbotin, S.A. (2013). Redescription of *Robustodorus megadorus* with molecular characterization and analysis of its phylogenetic position within the family Aphelenchoididae. *Journal of Nematology* 45, 237-252.

Skarmoutsos, G., Braasch, H. & Michalopoulou, H. (1998). *Bursaphelenchus hellenicus* sp. n. (Nematoda, Aphelenchoididae) from Greek pine wood. *Nematologica* 44, 623-629. DOI: 10.1163/005725998X00032

Skarmoutsos, H., Skarmoutsos, G., Kalapanida, M., Karageorgos, A., Mota, M. & Vieira, P. (2004). Surveying and recording of nematodes of the genus *Bursaphelenchus* in conifer forests in Greece and pathogenicity of the most important species. In: Mota, M. & Vieira, P. (Eds). *The pinewood nematode, Bursaphelenchus xylophilus. Proceedings of an International Workshop, University of Évora, Portugal, 20-22 August 2001. Nematology Monographs and Perspectives 1* (Series Editors: Cook, R. & Hunt, D.J.). Leiden, The Netherlands, Brill, pp. 113-126.

Subbotin, S.A., Sturhan, D., Chizhov, V.N., Vovlas, N. & Baldwin, J.G. (2006). Phylogenetic analysis of Tylenchida Thorne, 1949 as inferred from D2 and D3 expansion fragments of the 28S rRNA gene sequences. *Nematology* 8, 455-474. DOI: 10.1163/156854106778493420

Swofford, D.L. (2003). *PAUP*: phylogenetic analysis using parsimony (*and other methods), version 4.0b 10*. Sunderland, MA, USA, Sinauer Associates.

Tanaka, S.E., Tanaka, R., Akiba, M., Aikawa, T., Maehara, N., Takeuchi, Y. & Kanzaki, N. (2014). *Bursaphelenchus niphades* n. sp. (Tylenchina: Aphelenchoididae) amensally associated with *Niphades variegatus* (Roelofs) (Coleoptera: Curculionidae). *Nematology* 16, 259-281. DOI: 10.1163/15685411-00002763

Tanha Maafi, Z., Subbotin, S.A. & Moens, M. (2003). Molecular identification of cyst-forming nematodes (Heteroderidae) from Iran and a phylogeny based on the ITS sequences of rDNA. *Nematology* 5, 99-111. DOI: 10.1163/156854102765216731

Thompson, J.D., Gibson, T.J., Jeanmougin, F. & Higgins, D.G. (1997). The CLUSTAL_X windows interface: flexible strategies for multiple sequence alignment aided by quality analysis tools. *Nucleic Acids Research* 25, 4876-4882. DOI: 10.1093/nar/25.24.4876

Thong, C.H.S. & Webster, J.M. (1983). Nematode parasites and associates of *Dendroctonus* spp. and *Trypodendron lineatum* (Coleoptera: Scolytidae), with a description of *Bursaphelenchus varicauda* n. sp. *Journal of Nematology* 15, 312-318.

Tisserat, N., Cranshaw, W., Leatherman, D., Utley, C. & Alexander, K. (2009). Black walnut mortality in Colorado caused by the walnut twig beetle and thousand cankers disease. *Plant Health Progress*. DOI: 10.1094/PHP-2009-0811-01-RS

Tomalak, M. (2017). Parasitic association of the mycetophagous wood nematode, *Bursaphelenchus fraudulentus* with the honey fungus *Armillaria ostoyae*. *Forest Pathology* 47, e12325. DOI: 10.1111/efp.12325

Tomalak, M. & Filipiak, A. (2011). *Bursaphelenchus trypophloei* sp. n. (Nematoda: Parasitaphelenchinae) – an associate of the bark beetle, *Trypophloeus asperatus* (Gyll.) (Coleoptera: Curculionidae, Scolytinae), in aspen, *Populus tremula* L. *Nematology* 13, 619-636. DOI: 10.1163/138855410X532168

Tomalak, M. & Filipiak, A. (2019). *Bursaphelenchus michalskii* sp. n. (Nematoda: Aphelenchoididae), a nematode asso-

ciate of the large elm bark beetle, *Scolytus scolytus* Fabr. (Coleoptera: Curculionidae), in Dutch elm disease-affected elm, *Ulmus laevis* Pall. *Nematology* 21, 301-318. DOI: 10.1163/15685411-00003215

Tomalak, M., Worrall, J. & Filipiak, A. (2013). *Bursaphelenchus masseyi* sp. n. (Nematoda: Parasitaphelenchinae) – a nematode associate of the bark beetle, *Trypophloeus populi* Hopkins (Coleoptera: Curculionidae: Scolytinae), in aspen, *Populus tremuloides* Michx. affected by sudden aspen decline in Colorado. *Nematology* 15, 907-921. DOI: 10.1163/15685411-00002729

Torrini, G., Strangi, A., Mazza, G., Marianelli, L., Roversi, P.-F. & Kanzaki, N. (2019). Description of *Bursaphelenchus irokophilus* n. sp. (Nematoda Aphelenchoididae) isolated from *Milicia excelsa* (Welw.) C.C. Berg wood imported into Italy from Cameroon. *Nematology* 21, 957-969. DOI: 10.1163/15685411-00003268

Vrain, T.C. (1993). Restriction fragment length polymorphism separates species of the *Xiphinema americanum* group. *Journal of Nematology* 25, 361-364.

Wang, H.Y., Pan, C. & Chen, Y. (2004). A new record species of genus *Bursaphelenchus* Fuchs, 1937 (Nematoda: Parasitaphelenchidae) in *Pinus massoniana* from China. *Journal of Xiamen University* 5, 727-732.

Wang, H.Y., Yang, Z.F. & Zhang, S.S. (2005a). [Identification *of Bursaphelenchus rainulfi* from withered pine in Fujian province, China.] *Journal of Fujian Agricultural College of Forestry* 25, 221-224.

Wang, H.Y., Yang, Z.F. & Zhang, S.S. (2005b). Identification of *Bursaphelenchus rainulfi* Braasch, 2002, a new record for Japan. *Journal of Fujian Agriculture and Forestry University (Natural Science Edition)* 34, 158-161.

Wang, X., Gu, J., Maria, M., Fang, Y. & Li, H. (2018a). *Bursaphelenchus decraemerae* n. sp. (Tylenchina: Aphelenchoididae) found in packaging wood from the USA. *Nematology* 20, 119-131. DOI: 10.1163/15685411-00003129

Wang, X., Maria, M., Gu, J.F., Fang, Y., Wang, J.C. & Li, H. (2018b). *Bursaphelenchus geraerti* n. sp. (Tylenchina: Aphelenchoididae) found in packaging wood from the United Arab Emirates. *Nematology* 20, 583-595. DOI: 10.1163/15685411-00003163

Xu, Y., Gu, J.F., Zhang, J.C., Cui, J.X. & Zhang, Y.F. (2006). [Identification of *Bursaphelenchus rainulfi* in *Pinus massoniana* in Ningbo.] *Journal of Zhejiang Forest Science and Technology* 26, 37-39.

Ye, W.M., Giblin-Davis, R.M., Braasch, H., Morris, K. & Thomas, W.K. (2007). Phylogenetic relationships among *Bursaphelenchus* species (Nematoda: Parasitaphelenchidae) inferred from nuclear ribosomal and mitochondrial DNA sequence data. *Molecular Phylogenetics and Evolution* 43, 1185-1197. DOI: 10.1016/j.ympev.2007.02.006

Supplementary Table S1. *Bursaphelenchus* spp. of the *Abietinus* group. List of vectors and plant hosts.

Nematode species	Country and region	Vector	Associated plant	Reference
B. abietinus	Austria	*Pityokteines curvidens* (Germar) (type vector); *P. vorontzowi* (Jacobson), *P. spinidens* (Reitter) (Curculionidae: Scolytinae)	*Abies alba* Mill. (Pinales: Pinaceae)	Braasch & Schmutzenhofer (2000)
	Romania	unknown	*Picea abies* (L.) H. Karst; *Abies* spp. (Pinales: Pinaceae)	Calin *et al.* (2015)
B. antoniae	Portugal	*Hylobius* sp. (Curculionidae: Curculioninae)	*Pinus pinaster* Aiton (Pinales: Pinaceae)	Penas *et al.* (2006)
	USA: Massachusetts	*Hylobius* spp.	*Pinus strobus* L. (Pinales: Pinaceae)	Carta & Wick (2018)
B. chengi	packaging wood from Taiwan found in Nanjing (China)	unknown	Coniferous packaging wood	Li *et al.* (2008)
	China: Zhejiang	unknown	*Pinus taiwanensis* Hayata	Gu *et al.* (2009)
B. decraemerae	China and USA: Ningbo, China, from packaging wood made of *Pinus* sp. imported from the USA	unknown	*Pinus* sp. (Pinales: Pinaceae)	Wang *et al.* (2018a)
B. geraerti	Tianjin, China, packaging wood from the United Arab Emirates	"lower quality hardwood or coniferous wood"	*Pinus* sp. (Pinales: Pinaceae)	Wang *et al.* (2018b)
B. gerberae	Trinidad	*Rhynchophorus palmarum* (L.) (Curculionidae: Curculioninae)	*Cocos nucifera* L. (Arecales: Arecaceae)	Giblin-Davis *et al*. (2006)
	Vietnam	unknown	*Pinus* spp. (Pinales: Pinaceae)	Nguyen *et al.* (2016)
B. hellenicus	Greece, Germany, Portugal, Russia	*Tomicus piniperda* (L.) (syn. *Mielophilus piniperda* L.)	*Pinus brutia* Tenore; *Pinus sylvestris* L.; *Larix* sp. (Pinales: Pinaceae)	Skarmoutsos *et al.* (1998; 2004); Braasch *et al.* (1999); review in Ryss *et al.* (2005); Penas *et al.* (2008); d'Errico *et al.* (2015)
	Italy	unknown	*Pinus* spp. (Pinales: Pinaceae)	Carletti (2008)
	Turkey	unknown	*Pinus brutia* Tenore (Pinales: Pinaceae)	Akbulut *et al.* (2013)
	China: Yunnan province, Fujian province	unknown	*Pinus armandii* Franch.; *P. yunnanensis* Franch.; *Pinus massoniana* Lamb. (Pinales: Pinaceae)	Dan & Yu (2003); Qin & Pan (2005)

Supplementary Table S1. (Continued.)

Nematode species	Country and region	Vector	Associated plant	Reference
B. hylobianus	Russia: Magadan territory	*Hylobius albosparsus* Boheman (Coleoptera: Curculionidae)	*Larix dahurica* Turcz. (Pinales: Pinaceae)	Korenchenko (1980)
	Russia (intercepted in Germany)	unknown	*Larix sibirica* Ledeb.; *Pinus sylvestris* L. (Pinales: Pinaceae)	Braasch *et al.* (2001)
	Thailand	unknown	*Pinus merkusi* Jungh & de Vriese (Pinales: Pinaceae)	Braasch & Braasch-Bidasak (2002)
	Portugal	*Hylobius* sp. (Coleoptera: Curculionidae)	*Pinus pinaster* Aiton (Pinales: Pinaceae)	Penas *et al.* (2004)
	Spain	unknown	*Pinus radiata* D. Don (Pinales: Pinaceae)	Arias *et al*. (2004); Escuer *et al.* (2004)
	China	unknown	*Pinus massoniana* Lamb. (Pinales: Pinaceae)	Wang *et al.* (2004)
	China (intercepted from Japan)	unknown	packaging wood	Gu *et al.* (2006)
B. irokophilus	Logs from Cameroon arriving in Tuscany, Italy	unknown	*Milicia excelsa* (Welw.) C.C. Berg (Rosales: Moraceae)	Torrini *et al.* (2019)
B. juglandis n. sp.	USA: California	*Pityophthorus juglandis* Blackman	*Juglans hindsii* × (*J. nigra* × *J. hindsii*/*J. californica* (Fagales: Juglandaceae)	This paper
B. niphades	Japan: Tokyo, Akita, Nagano, Ibaraki, Yamanashi	*Niphades variegatus* (Roelofs) (Curculionidae: Curculioninae)	*Pinus densiflora* Sieb. & Zucc.; *P. thunbergii* Parl.; *Abies veitchii* Lindl.; *A. firma* Sieb. & Zucc.). (Pinales: Pinaceae)	Tanaka *et al.* (2014)
B. parantoniae	Ningbo, China, packaging wood from Belgium	unknown	*Pinus* sp. (Pinales: Pinaceae)	Maria *et al.* (2015)
B. pityogeni	USA: New Mexico	*Pityogenes carinulatus* (LeConte)	*Pinus ponderosa* P. & C. Lawson (Pinales: Pinaceae)	Massey (1974)
B. rainulfi	Malaysia: Kuala Lumpur	Curculionidae: Scolytinae, species unknown	*Pinus caribaea* Morelet (Pinales: Pinaceae)	Braasch & Burgermeister (2002)
	China: Zhejiang, Fujian	unknown	*Pinus massoniana* Lamb. (Pinales: Pinaceae)	Wang *et al.* (2005a); Gu *et al.* (2006); Xu *et al.* (2006); Jiang *et al*. (2007)
	Intercepted from Chinato, Italy (Trieste)	unknown	*Callitris columellaris* F. Mueller (Cupressaceae, packaging wood)	Ambrogioni *et al*. (2003)
	South Korea, Germany	unknown	Packaging wood	Li *et al.* (2009)
	Japan	unknown	*Pinus* sp. as packaging wood	Wang *et al.* (2005b)
	Vietnam	unknown	*Pinus* spp. (Pinales: Pinaceae)	Nguyen *et al.* (2016)
B. sakishimanus	Japan: Okinawa	*Dorcus titanus sakishimanus* Nomura (Lucanidae)	*Ananas comosus* (L.) Merr. (Poales: Bromeliaceae)	Kanzaki *et al.* (2015)

Supplementary Table S1. (Continued.)

Nematode species	Country and region	Vector	Associated plant	Reference
B. sinensis	China (wood intercepted in Austria)	unknown	*Pinus* sp. (Pinales: Pinaceae)	Palmisano *et al*. (2004)
	Japan	unknown	*Pinus thunbergii* Parl. (Pinales: Pinaceae)	Kanzaki & Futai (2007)
	Vietnam	unknown	*Pinus* spp. (Pinales: Pinaceae)	Nguyen *et al.* (2016)
B. varicauda	Canada: British Columbia	*Dendroctonus pseudotsugae* Hopkins (Curculionidae: Scolytinae)	*Pseudotsuga* sp. (Pinales: Pinaceae)	Thong & Webster (1983)
B. willi	USA: New Mexico	*Dendroctonus valens* LeConte (Curculionidae: Scolytinae)	*Pinus ponderosa* P. & C. Lawson (Pinales: Pinaceae)	Massey (1974)